

VIII. ATMOSPHERIC RESULTS, PART II. STATISTICAL ANALYSES

A. Correlation Between Pollutant Concentration

Table 14 includes a Pearson's correlation coefficient matrix between aerosol constituents, O_3 , R.H. and T. Notable features of these data include the absence of a significant correlation between HNO_3 and fine or coarse nitrate (see Discussion, Section VII G). Ammonia showed some correlation with fine nitrate ($r = 0.58$). Fine mass is relatively strongly correlated with particulate NH_4^+ ($r = 0.85$), organic carbon ($r = 0.75$), and fine elemental C ($r = 0.68$).

B. Correlation Between Single Pollutant Concentrations and Visibility Parameters

Average compositions of fine particle fractions and the correlation between the dry particle scattering coefficient, b_{sp} , and individual aerosol constituents, NH_3 and HNO_3 for each site, are shown in Table 15. Highest correlations were observed with fine sulfate, fine nitrate, total NH_4^+ and total organic carbon. Nitric acid and NH_3 showed only weak correlation. At San Jose and Riverside, nitrate was much more abundant than sulfate while the reverse was true in Los Angeles. Nitrate and NH_4^+ generally showed the highest correlation with b_{sp} .

A correlation coefficient matrix between the four visibility parameters and individual pollutant, relative humidity and temperature is given in Table 16 for all sites combined. The parameter b_{ag} , due to absorption by NO_2 , did not show high correlation with any of the variables listed. The particle absorption coefficient correlated well only with elemental carbon, with highest value for the fine C_e . The parameter b_{sw} , used to estimate the scattering of particle-bound water, showed moderate correlation with fine mass, fine sulfate and NH_4^+ and much weaker correlation with relative humidity (see Section V). The highest

Table 14

PEARSON CORRELATION COEFFICIENTS BETWEEN AEROSOL CONSTITUENTS, OZONE AND METEOROLOGICAL PARAMETERS

	$\overline{FSO_4}$	$\overline{CSO_4}$	$\overline{PNO_3}$	$\overline{CNO_3}$	$\overline{HNO_3}$	$\overline{NH_4^+}$	$\overline{NH_3}$	$\overline{FC_e}$	$\overline{CC_e}$	$\overline{C_o}$	\overline{R}	$\overline{O_3}$	\overline{RH}	\overline{T}
$\overline{FSO_4}$	1.0													
$\overline{CSO_4}$	0.52	1.0												
$\overline{PNO_3}$	0.33	0.36	1.0											
$\overline{CNO_3}$	0.32	0.63	0.52	1.0										
$\overline{HNO_3}$	0.54	0.31	0.29	0.22	1.0									
$\overline{NH_4^+}$	0.75	0.58	0.76	0.57	0.44	1.0								
$\overline{NH_3}$	- 0.03	0.11 ^c	0.58	0.17 ^c	0.02 ^c	0.41	1.0							
$\overline{FC_e}$	0.22	0.35	0.52	0.51	0.46	0.43	0.02 ^c	1.0						
$\overline{CC_e}$	0.29	0.36	0.49	0.44	0.60	0.45	0.10 ^c	0.81	1.0					
$\overline{C_o}$	0.44	0.43	0.64	0.60	0.64	0.68	0.32	0.72	0.75	1.0				
\overline{R}	0.76	0.57	0.67	0.57	0.61	0.85	0.14	0.68	0.66	0.75	1.0			
\overline{RFMass}	0.38	---	0.30	---	0.31	0.31	- 0.09 ^c	0.39	---	0.15	---	1.0		
$\overline{O_3}$	0.34	0.18	0.59	0.15 ^c	0.39	0.57	0.65	- 0.01 ^c	0.20 ^c	0.52	0.36	---	1.0	
\overline{RH}	0.20 ^c	0.14	- 0.22 ^c	- 0.06 ^c	- 0.26	- 0.04 ^c	- 0.42	- 0.05 ^c	- 0.16 ^c	- 0.43	0.04 ^c	---	- 0.47	1.0
\overline{T}	0.15 ^c	0.11 ^c	0.43	0.27	0.45	0.35	0.55	0.14 ^c	0.31	0.63	0.27	---	- 0.72	- 0.83

a. Except as noted, for all correlations n = 103-109. "C" and "P" indicates fine and coarse, respectively. R = residual fine mass (i.e. other than SO₄, NO₃, NH₄).

b. n = 88 to 92

c. Not significantly different from zero at p = 0.95

Table 15

CORRELATION BETWEEN FINE AEROSOL CONSTITUENTS (OR AEROSOL PRECURSORS) AND b_{sp}

Species	San Jose		Riverside		Los Angeles		Overall	
	% of FMass	r	% of FMass	r	% of FMass	r	% of FMass	r
FSO_4^-	7.92	0.80	13.2	0.66	22.0	0.60	16.3	0.71
$FN0_3^-$	16.1	0.88	25.7	0.86	13.3	0.84	18.7	0.80
NH_4^+	1.41	0.88	11.6	0.69	8.7	0.87	8.60	0.86
FC_e	7.34	0.74	4.75	0.18 ^c	5.6	0.54	5.57	0.53
C_o^d	45.1 ^d	0.71	33.4 ^d	0.36	30.9 ^d	0.75	34.1 ^d	0.70
R^b	22.1	0.12	11.4	0.30	19.6	0.67	16.8	0.55
NH_3	---	0.34 ^c	---	0.54	---	0.24 ^c	---	0.33
HNO_3	---	0.43	---	0.53	---	0.44	---	0.57

a. C and F indicate coarse and fine, respectively

b. R indicates residual fine mass, (fine mass) - (SO_4) - (NO_3^-) - (calc. fine NH_4^+)

c. Not significantly different from zero at $p = 0.95$

d. Total organic carbon calculated assuming all C_o in fine fraction: Estimated to be too high by up to a factor of two

Table 16

PEARSON CORRELATION COEFFICIENTS BETWEEN VISIBILITY PARAMETERS
INDIVIDUAL POLLUTANTS AND METEOROLOGICAL PARAMETERS

Parameter	$\overline{FSO_4}$	$\overline{CSO_4}$	$\overline{FNO_3}$	$\overline{CNO_3}$	$\overline{HNO_3}$	$\overline{NH_4^+}$	$\overline{NH_3}$	\overline{FC}	\overline{CC}	\overline{CO}	$\overline{PM_{10}}$	$\overline{O_3}$	\overline{RH}	\overline{T}
b _{ag}	0.49	0.58	0.47	0.55	0.31	0.62	0.12 ^a	0.55	0.57	0.46	0.65	0.09 ^a	0.15 ^a	0.10 ^a
b _{sp}	0.71	0.56	0.80	0.47	0.57	0.86	0.33	0.53	0.55	0.70	0.90	0.52	0.10 ^a	0.27
b _{ap}	0.19	0.31	0.41	0.39	0.43	0.32	- 0.06 ^a	0.92	0.76	0.64	0.62	- 0.02 ^a	- 0.03 ^a	0.13 ^a
b _{sw}	0.74	0.54	0.48	0.43	0.29	0.73	0.05 ^a	0.27	0.31	0.32	0.64	0.19 ^a	0.41	- 0.06 ^a

a. Not significantly different from zero at p = 0.95

correlation was that between the dry particle scattering coefficient and fine aerosol mass ($r = 0.90$). This is illustrated in Figure 33.

C. Multiple Regression Analyses Between Particle Scattering Coefficient and Pollutant Concentrations

Multiple regression analysis was performed between the dry particle scattering coefficient, b_{sp} , and the concentration of chemical species with equations of the form:

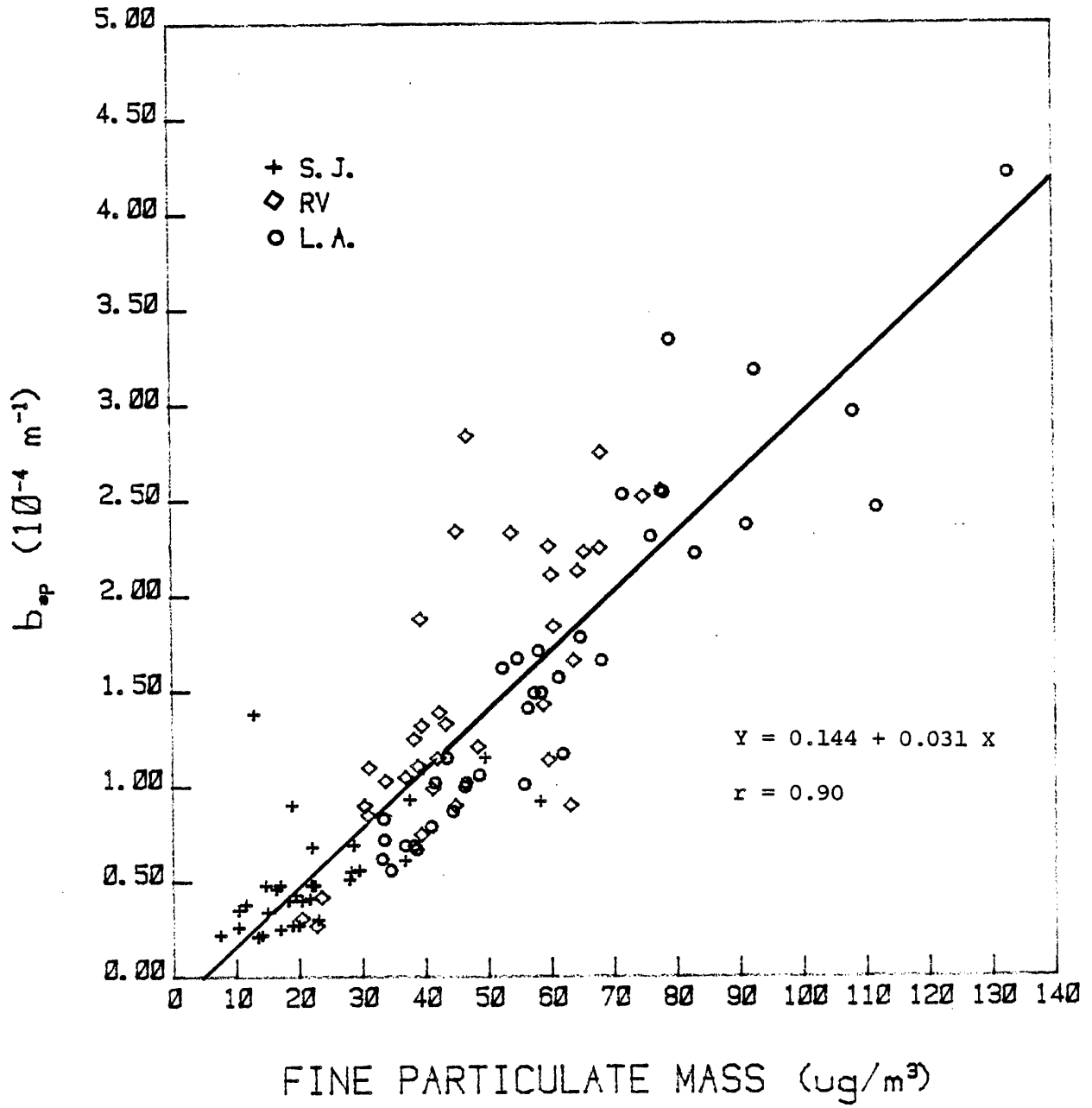
$$b_{sp} = a + b (F\overline{SO}_4) + c (C\overline{SO}_4) + d (F\overline{NO}_3) + e (C\overline{NO}_3) + f (F\overline{C}_e) + g (C\overline{C}_e) + h\overline{C}_o + iR$$

Where F = fine, C = Coarse and R = residual fine mass (material other than $F\overline{SO}_4$, $F\overline{NO}_3$, $F\overline{C}_e$ and $F\overline{NH}_4^+$)

The coefficients b, c can be considered the scattering efficiency per unit concentration ($\mu\text{g}/\text{m}^3$) of the species. The weight concentrations in the equation are those measured for the anions, alone. This contrasts with a number of prior studies for which \overline{NO}_3 and \overline{SO}_4 were assumed to be present as their ammonium salts, and weight concentrations calculated accordingly. The resulting coefficients from such studies are, therefore, lower by a factor representing the weight fraction of the anion in the compound.

It should also be recognized that the scattering efficiency should vary with particle surface area. Thus as size distributions change the scattering efficiencies per unit concentration should change as well. In Table 14, coarse and fine sulfate show moderate correlation ($r = 0.52$), and that between coarse and fine elemental carbon is relatively strong ($r = 0.81$). Multiple regressions involving these components are made unstable by such co-linearity and yield increased standard deviations as a result. The extent to

Figure 33. Scattering Diagram of Fine Particulate Mass Against the Dry Particle Scattering Coefficient



which such co-linearity has influenced the coefficients for these components in multiple regression is unclear.

The coefficients for the above regression equation and the influence of eliminating one or two of the variables are shown in Table 17. Notable features of these data include:

1. Relatively constant coefficients for the intercept, FSO_4^- , FNO_3^- , and FC_e .
2. Somewhat higher scattering efficiencies per unit mass for fine nitrate compared to fine sulfate in contrast to most previously published studies. This reflects, at least in part, the elimination of the artifact particulate nitrate error caused by the collection of HNO_3 on glass fiber, cellulose ester, and other filter types.
3. The extraordinarily high coefficient for coarse sulfate. We suspect that this material may be functioning as a surrogate for sea salt aerosol; sea salt chloride is about seven times the concentration of sea salt sulfate, which probably exists to significant degree in the coarse fraction. Omitting coarse sulfate from the regression (Model 5) increased slightly the coefficient for fine sulfate without affecting that for fine nitrate.
4. Fine elemental carbon similar in scattering efficiency to sulfate.
5. A nearly insignificant coefficient for organic carbon, based on hi-vol sampling without size fractionation.

Table 17

MULTIPLE REGRESSION ANALYSIS BETWEEN AEROSOL CONSTITUENTS AND $b_{sp}^{a,b,d}$

Constituent:	FSO_4^-	CSO_4^-	FNO_3^-	CNO_3^-	FC_e	CC_e	C_o	R		
Coefficient:	<u>a</u>	<u>b</u>	<u>c</u>	<u>d</u>	<u>e</u>	<u>f</u>	<u>g</u>	<u>h</u>		
Model	<u>r²</u>									
1	- 0.15 (.08)	0.049 (.006)	0.134 (.050)	0.063 (.005)	- 0.012 (.008)	0.045 (.025)	0.023 (.087)	0.013 (.008)	0.004 (.004)	0.915
2	- 0.14 (.07)	0.051 (.005)	0.132 (.049)	0.065 (.005)	- 0.01 ^c (.008)	0.054 (.023)	0.035 ^c (.086)	0.01 ^c (.007)	---	0.914
3	- 0.14 (.07)	0.051 (.006)	0.090 (.040)	0.063 (.005)	---	0.048 (.022)	---	0.01 ^c (.007)	0.003 ^c (.004)	0.912
4	- 0.11 ^c (.07)	0.053 (.005)	0.090 (.040)	0.065 (.005)	---	0.049 (.023)	0.060 ^c (.084)	0.006 ^c (.007)	---	0.912
5	- 0.07 (.07)	0.056 (.005)	---	0.065 (.005)	0.001 (.007)	0.044 (.026)	0.060 (.089)	0.008 (.008)	0.003 (.004)	0.908

a. $b_{sp} = a + b (FSO_4^-) + c (CSO_4^-) + d (FNO_3^-) + e (CNO_3^-) + f (FC_e) + g (CC_e) + h (C_o) + i (R)$

b. See Table 15 for explanation of abbreviations. Values in parenthesis are standard deviations.

c. Not significantly different from zero at $p = 0.95$

d. Units are $10^{-4} m^{-1} / \mu g \cdot m^{-3}$. For example, 0.049 in these units corresponds to $4.9 m^2/g$.

D. Average Contributions of Aerosol Species to the Scattering and Total Extinction Coefficients

The total extinction coefficient, b'_{ext} , can be expressed as the total of b_{sp} , b_{sw} , b_{ap} , and b_{ag} . Employing the best fit regression equations, b'_{ext} can be expressed as:

$$b'_{\text{ext}} (\times 10^4) = - 0.14 + 0.051 (\text{FSO}_4) + 0.064 (\text{FNO}_3) + 0.049 (\text{FC}_e) + 0.11 (\text{CSO}_4) \\ + 0.081 (\text{FSO}_4) \mu + 0.062 (\text{FNO}_3) \mu + 0.116 (\text{FC}_e) + 3.3 \times 10^{-3} \text{NO}_2$$

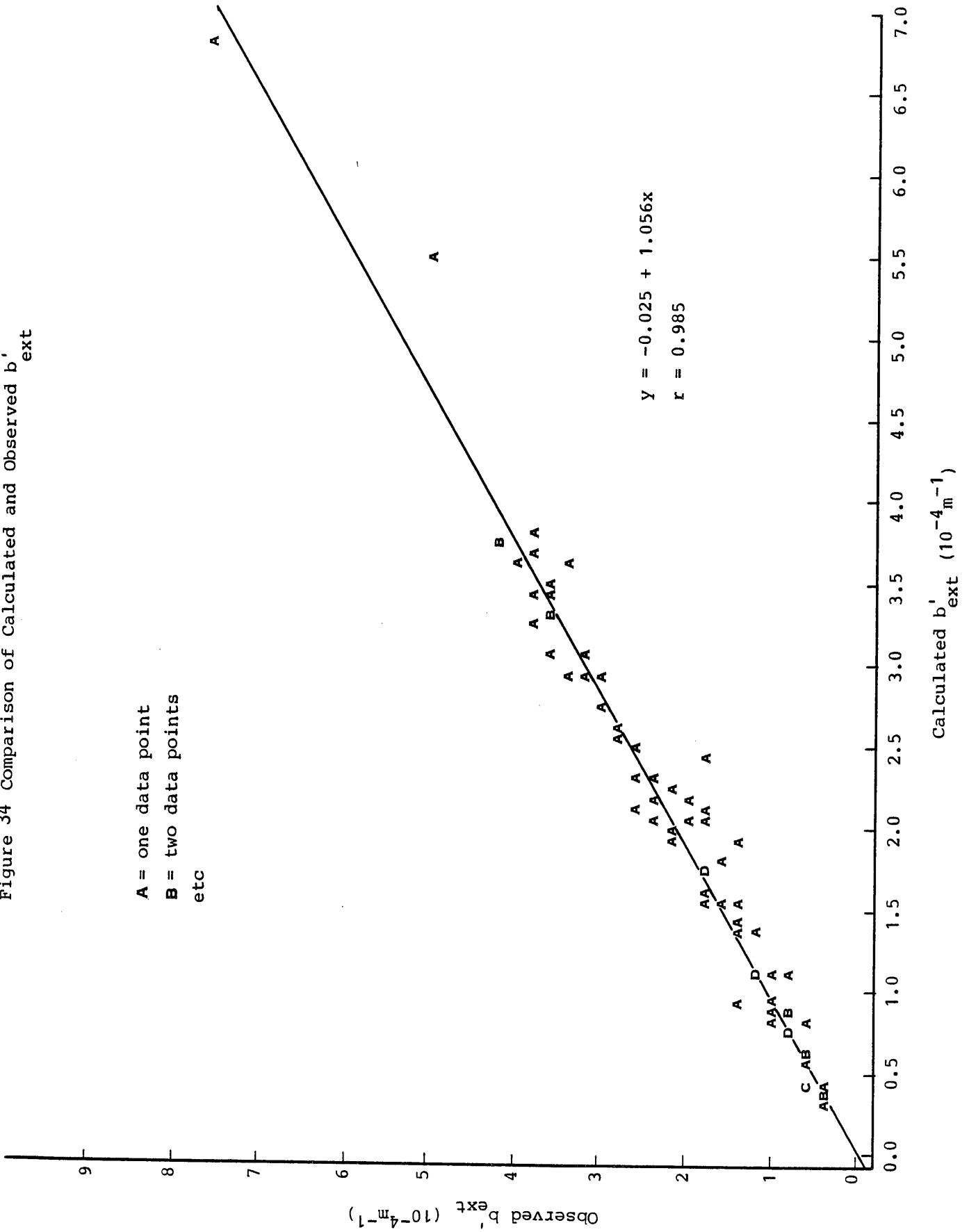
where $\mu = \text{RH}/100$ and NO_2 is in ppb.

The coefficients for the b_{sp} regression equation the first 5 terms were calculated from Table 17 as the mean values for the models 1-4. The equation for b_{sw} (terms 6 and 7) is taken from Table 9 and that for b_{ap} (term 8), from Section IV. The final term is that for b_{ag} (Reference 6).

The internal consistency of this regression equation can be assessed by comparing b'_{ext} as calculated above, to the value of b'_{ext} using directly measured values for b_{sp} , b_{sw} and b_{ap} . The total of these parameters plus 3.3×10^{-3} (NO_2) is here termed the observed extinction coefficient ($b'_{\text{ext}})_{\text{obs}}$. Figure 34 is a scatter diagram of observed against calculated extinction coefficients. The correlation coefficient is 0.96 and the slope indicates average agreement within 6%.

Using the mean 4-hour average concentrations for the chemical species judged to be significant contributors to b_{sp} and b'_{ext} , the

Figure 34 Comparison of Calculated and Observed b'_{ext}



mean proportions due to each species are shown in Table 18. The contribution due to nitrate- and sulfate-related water are here included as part of the contributions of these species. Nitrate is the largest single contributor to both optical parameters, providing, on average for the three sites, over half of the light scattering and over a third of the extinction. Sulfate is second in importance. Because of substantial differences between sites, these conclusions will be site dependent.

Fine elemental carbon contributes to extinction by both scattering and absorption. In total it provided on average, nearly 20% of the extinction. Coarse sulfate (or species proportional to it such as sea salt) appears to contribute nearly 14% of the light scattering and 7% of the extinction. Insignificant factors from analysis of the current data include organic carbon, coarse C_e , coarse nitrate and residual fine mass. Absorption due to NO_2 represented 8% of the mean extinction coefficient.

E. Comparison of Present Results with those for General Motors' Denver Visibility Study (6)

Denver aerosol during winter sampling was dominated by carbonaceous material, believed to be from residential wood burning, with elemental carbon representing 15% of fine mass compared to 7% here. Nitrate was more abundant than sulfate but the difference was only a factor of 1.4 compared to 2.0 in the present work. On average particle light absorption, b_{ap} , represented about 29% of the extinction coefficient in Denver compared to 22, 9 and 12% at San Jose, Riverside and downtown Los Angeles, respectively. This is consistent with the lower proportion of C_e in the present work.

The GM work yielded scattering efficiencies per mass concentration of $(NH_4)_2SO_4$ of 6.6 and for NH_4NO_3 , 2.8 m^2/g . Expressed as $SO_4^{=}$ and NO_3^- , these correspond to 9.1 and 3.6 m^2/g , respectively. Thus sulfate was more efficient per unit mass than nitrate as collected

Table 18

AVERAGE PERCENT CONTRIBUTIONS OF CHEMICAL SPECIES TO THE PARTICLE SCATTERING COEFFICIENT, b_{sp} , AND TO THE EXTINCTION COEFFICIENT, b'_{ext} ^a

<u>Species</u>	<u>Mean % of b_{sp}</u>	<u>Mean % of b'_{ext}</u>
FSO_4^-	36.0	30.0
FNO_3^-	52.1	36.2
CSO_4^-	13.9	6.7
CNO_3^-	ca.0	ca.0
FC_e	11.9	5.7 (scattering) 13.5 (absorption)
CC_e	ca.0	ca.0
C_o	ca.0	ca.0
R	ca.0	ca.0
NO_2	--	8.0

a. b'_{ext} refers to the total extinction coefficient minus the Rayleigh scattering coefficient, b_{sg} .

by Teflon filters. Both organic and elemental carbon were significant contributors to b_{sp} in the Denver study, similar to nitrate in efficiency.

The most significant difference between results for the two studies is the relative efficiency of sulfate and nitrate for light scattering. Since particulate nitrate sampling in Denver was done with Teflon filters, the resulting nitrate values should be lower limits to the true value. Accordingly, the efficiency per unit mass of nitrate should be an upper limit value. Thus sampling errors do not explain the difference between these studies. Hasan and Dzubay (56) confirmed the multiple regression analysis results of Groblicki et al. using the Denver data. However, they found that calculated values of the scattering efficiency per unit mass for nitrate, based on measured size distributions and Mie theory, were 38% higher than those observed in Denver. They concluded that extinction coefficients apportioned to specific chemical species were uncertain by a factor of two. Further work is needed to reconcile the findings of these studies in this respect.

F. Comparison of the Present Results to those Reported by Trijonis et al

The present results may be compared to those of Trijonis et al (48). These authors have discussed extensively the relative magnitude of the scattering efficiencies per unit mass for sulfate and nitrate. Their study was restricted to hi-vol filter data obtained, in nearly all cases, with glass fiber filters. Thus they acknowledged that the coefficient for nitrate is especially uncertain because of the potential formation of artifact nitrate. Using multiple regression analysis, they found nitrate to be relatively more efficient in light scattering than sulfate in Northern California and the reverse, in Southern California. The temperature dependence of NH_4NO_3 dissociation to HNO_3 leading to greater HNO_3 retention on filters in Southern California was used to rationalize this. In

addition, sulfate was noted to be an especially efficient source of light scattering when present in relatively large particle size, 0.5 to 1.0 μm . Similar to the current study results for C_0 , a statistically significant ($p = 0.95$) scattering efficiency for benzene-soluble organics was not observed.

REFERENCES

1. R. J. Charlson. Atmospheric Visibility Related to Aerosol Mass Concentration. *Environ. Sci. and Technol.* 3 913-918 (1969).
2. D. M. Roessler and F. R. Faxvog. Visibility in Absorbing Aerosols. *Atmos. Environ.* 15 151-155 (1981).
3. J. Trijonis. Visibility in California. Final Report to the California Air Resources Board for ARB Contract A7-181-30 (1980).
4. G. M. Hidy et al. Characterization of Aerosols in California, Vol. I. Final Report to the California Air Resources Board for ARB Contract 358.
5. W. H. White and P. T. Roberts. On the Nature and Origins of Visibility-Reducing Aerosols in the Los Angeles Air Basin. *Atmos. Environ.* 11 803-812 (1977).
6. P. J. Groblicki, G. T. Wolff and R. J. Countess. Visibility Reducing Species in the Denver "Brown Cloud", Part 1. Relationships Between Extinction and Chemical Composition (1980). *Atmos. Environ.* 15, 2473-2454 (1981).
7. G. R. Cass. The Relationship Between Sulfate Air Quality and Visibility At Los Angeles. EQL Memorandum No. 18. California Institute of Technology (1976).
8. B. J. Leaderer, T. R. Holford and J. A. J. Stolwijk. Relationship Between Sulfate Aerosol and Visibility. *J. Air Poll. Cont. Assoc.* 29 154 (1979).

9. B. R. Appel, E. L. Kothny, E. M. Haik, G. M. Hidy and J. J. Wesolowski. Sulfate and Nitrate Data from the California Aerosol Characterization Experiment (ACHEX). *Environ. Sci. and Technol.* 12 418-425 (1978).
10. J. N. Pitts, Jr., D. Grosjean, B. Shortridge, G. Doyle, J. Smith, T. Mischke and D. Fitz. The Nature, Concentration and Size Distribution of Organic Particulates in the Eastern Part of the Southern California Air Basin. Presented at the 171st ACS Meeting, New York. April 1976.
11. A. Albagli, H. Oja and L. Dubois. Size Distribution Patterns of Polycyclic Aromatic Hydrocarbons in Airborne Particulate. *Environmental Letters* 6 241-254 (1974).
12. E. M. Patterson. Optical Properties of Urban Aerosols Containing Carbonaceous Materials. Conference on Carbonaceous Particles in the Atmosphere. Berkeley, CA. March 1978.
13. J. Heintzenberg. Light Absorption Measurements in Europe. Conference on Carbonaceous Particles in the Atmosphere. Berkeley, CA. March 1978.
14. R. E. Weiss, A. P. Waggoner, D. J. Thorsell, J. S. Hall, L. A. Riley and R. J. Charlson. On the Nature of Light Absorbing Aerosols. Conference on Carbonaceous Particles in the Atmosphere. Berkeley, CA. March 1978.
15. R. L. Williams and D. P. Chock. Characterization of Diesel Particulate Exposure. General Motors Research Publication GMR-3177 (1979).
16. R. W. Coutant. Effect of Environmental Variables on Collection of Atmospheric Sulfate. *Environ. Sci. and Technol.* 11 873-878 (1977).
17. B. R. Appel, Y. Tokiwa, S. M. Wall, E. M. Hoffer, M. Haik and J. J. Wesolowski. Effect of Environmental Variables and Sampling Media on the Collection of Atmospheric Sulfate and Nitrate. Final Report ARB Contract 5-1032 (1978).

18. B. R. Appel, E. M. Hoffer, E. L. Kothny, Y. Tokiwa and J. J. Wesolowski. Sampling and Analytical Problems in Air Pollution Monitoring. EPA Cooperative Agreement No. CR 806734-02-0. First Quarterly Progress Report (1980).
19. C. W. Spicer and P. Schumacher. Interference in Sampling Atmospheric Particulate Nitrate. *Atmos. Environ.* 11 873-876 (1977).
20. B. R. Appel, S. M. Wall, Y. Tokiwa and M. Haik. Interference Effects in Sampling Particulate Nitrate in Ambient Air. *Atmos. Environ.* 13 319-325 (1981)
21. B. R. Appel, Y. Tokiwa and M. Haik. Sampling of Nitrates in Ambient Air. *Atmos. Environ.* 15 283-289 (1981).
22. A. B. Harker, L. W. Richards and W. E. Clark. The Effects of Atmospheric SO₂ Photochemistry upon Observed Nitrate Concentrations in Aerosols. *Atmos. Environ.* 11 87-91 (1977).
23. B. R. Appel and Y. Tokiwa. Atmospheric Particulate Nitrate Sampling Errors Due to Reactions with Particulate and Gaseous Strong Acids. *Atmos. Environ.* 15 1087-1089 (1981).
24. C. Pupp, R. C. Lao, J. J. Murray and R. F. Pottie. Equilibrium Vapour Concentrations of Some Polycyclic Aromatic Hydrocarbons, As₄O₆ and SeO₂ and the Collection Efficiencies of These Air Pollutants. *Atmos. Environ.* 8 915-925 (1974).
25. H. Della Fiorentina, J. De Graeve and F. De Wiest. Determination par Spectrometrie Infrarouge de la Matiere Organique Non Volatile Associee aux Particules en Suspension dans L'Air - I. Choix des Conditions Operatoires. *Atmos. Environ.* 9 513-516 (1975).
26. H. Della Fiorentina, F. De Wiest and J. De Graeve. Determination par Spectrometrie Infrarouge de la Matiere Organique Non Volatile Associee

aux Particules en Suspension dans L'Air-II. Facteurs Influençant L'Indice Aliphatique. Atmos. Environ. 9 517-522 (1975).

27. F. De Wiest and H. Della Fiorentina. Suggestions for a Realistic Definition of an Air Quality Index Relative to Hydrocarbonaceous Matter Associated with Airborne Particles. Atmos. Environ. 9 951-954 (1975).
28. W. Cautreels and K. Van Cauwenberghe. Experiments on the Distribution of Organic Pollutants Between Airborne Particulate Matter and the Corresponding Gas Phase. Atmos. Environ. 12 1133-1141 (1978).
29. B. R. Appel, E. M. Hoffer, E. L. Kothny, S. M. Wall, M. Haik and R. L. Knights. Analysis of Carbonaceous Material in Southern California Atmospheric Aerosols, 2. Environ. Sci. and Technol. 13 98-104 (1979).
30. R. E. Clement and F. W. Karasek. Sample Composition Changes in Sampling and Analysis of Organic Compounds in Aerosols. Intern. J. Environ. Anal. Chem. 7 109-120 (1979).
31. J. König, W. Funcke, E. Balfanz, B. Grosch and F. Pott. Testing a High Volume Air Sampler for Quantitative Collection of Polycyclic Aromatic Hydrocarbons. Atmos. Environ. 14 609-613 (1980).
32. J. Peters and B. Seifert. Losses of Benzo(a)Pyrene Under the Conditions of High-Volume Sampling. Atmos. Environ. 14 117-119 (1980).
33. Gary P. Schwartz, Joan M. Daisey and Paul J. Liroy. Effect of Sampling Duration on the Concentration of Particulate Organics Collected on Glass Fiber Filters. Am. Ind. Hyg. Assoc. J. 42 258-263 (1981).
34. B. R. Appel, J. Hsu, Y. Tokiwa and J. J. Wesolowski. Characterization of Organic Particulate Matter-II. Final Report for ARB Contract No. A9-O74-31 (1982).

35. C. I. Lin, M. Baker and R. J. Charlson. Absorption Coefficient of Atmospheric Aerosol: A Method for Measurement. *Applied Optics* 12 1356-1363 (1973).
36. R. W. Shaw, Jr., R. K. Stevens, J. Bowermaster, J. W. Tesch, and E. Tew. Measurements of Atmospheric Nitrate and Nitric Acid: The Denuder Difference Experiment. *Atmos. Environ.* 16, 845-853 (1981).
37. B. R. Appel, S. M. Wall, Y. Tokiwa and M. Haik. Simultaneous Nitric Acid, Particulate Nitrate and Acidity Measurements in Ambient Air. *Atmos. Environ* 14 549-554 (1980).
38. R. J. Countess, S. H. Cadle, P. J. Groblicki and G. T. Wolff. Chemical Analysis of Size-Segregated Samples of Denver's Ambient Particulate. *J. Air Poll. Cont. Assoc.* 31 247-252 (1981).
39. T. Novakov. "Soot in the Atmosphere," in *Particulate Carbon: Atmospheric Life Cycle*, C. T. Wolff and R. L. Klimisch, Editors (1982).
40. B. R. Appel, Y. Tokiwa, and E. L. Kothny. Sampling of Carbonaceous Particles in the Atmosphere. *Atmos. Environ.* 17, 1787 (1983).
41. C. I. Lin, M. Baker and E. J. Charlson. Absorption Coefficient of Atmospheric Aerosol: A Method for Measurement. *Applied Optics* 12, 1356-1363 (1973).
42. H. Rosen, A. D. A. Hansen, L. Gundel and T. Novakov. *Applied Optics* 17, 3859 (1978).
43. R. E. Weiss, A. P. Waggoner, R. J. Charlson, D. L. Thorsell, J. S. Hall and L. A. Riley. Studies of the Optical, Physical and Chemical Properties of Light Absorbing Aerosols. Proceedings, "Carbonaceous Particles in the Atmosphere", T. Novakov, Ed. Lawrence Berkeley Laboratory, University of California, March 1978, LBL-9037, CONF-7803101, UC-11

44. R. K. Stevens, W. A. McClenny, T. G. Dzubyay, M. A. Mason and W. J. Courtney. "Analytical Methods to Measure the Carbonaceous Content of Aerosols", in Particulate Carbon: Atmospheric Life Cycle. G. T. Wolff and R. L. Klimisch, Editors (1982).
45. "Light Absorption by Aerosol Particles", H. E. Gerber and E. E. Hindman, Editors, Spectrum Press, Hampton, VA (1982).
46. M. Sadler, R. J. Charlson, H. Rosen and T. Novakov, An Intercomparison of the Integrating Plate and the Laser Transmission Method for Determination of Aerosol Absorption Coefficients. Lawrence Berkeley Laboratory Report 11176 (1980), and Atmos. Environ. 15, 1265 (1981).
47. R. E. Weiss, private communication (1981).
48. J. Trijonis, G. Cass, G. McRae, Y. Horie, W. -Y. Lim, N. Chang and T. Cahill. "Analysis of Visibility/Aerosol Relationships and Visibility Modeling/Monitoring Alternatives for California. Final Report to California Air Resources Board. Contract A9-103-31 (1982)
49. S. H. Cadle, P. J. Groblicki and D. P. Stroup. An Automated Carbon Analyzer for Particulate Samples. Anal. Chem. 52, 2201-2206 (1980).
50. A. D. Clarke and A. P. Waggoner. App. Opt. 21, 398 (1982).
51. G. T. Wolf, M. A. Ferman, N. A. Kelly, D. P. Stroup and M. S. Ruthkosky, Paper 82-11M.2. Presented at the 75th Annual Meeting of the Air Poll. Cont. Assoc., New Orleans, June 1982.
52. B. R. Appel, Y. Tokiwa, S. Wall, E. M. Hoffer, M. Haik and J. J. Wesolowski. Effects of Environmental Variables and Sampling Media on the Collection of Atmospheric Sulfate and Nitrate. Final Report to the California Air Resources Board. Contract No. ARB 5-1032 (1978).

53. A. W. Stelson, S. K. Friedlander and J. H. Seinfeld. A Note on the Equilibrium Relationship between Ammonia and Nitric Acid and Particulate Ammonium Nitrate. *Atmos. Environ.* 13, 369-371 (1979).
54. D. Grosjean. Distribution of Nitrogenous Pollutants During Photochemical Smog Episodes. Paper presented at the 75th Annual Meeting of the Air Pollution Control Association, New Orleans (1982).
55. Z. Yasa, N. M. Amer, H. Rosen, A.D. A. Hansen, and T. Novakov. Photoacoustic Investigation of Urban Aerosol Particles. *Appl. Optics* 18, 2528-2530 (1979).
56. H. Hansen and T. G. Dzubay. Apportioning Light Extinction Coefficients to Chemical Species in Atmospheric Aerosol. *Atmos. Environ.* (In Press) 1983.
57. A. P. Waggoner, R. E. Weiss, N. C. Ahlquist, D. S. Covert, S. Will and R. J. Charlson. Optical Characteristics of Atmospheric Aerosols. *Atmos. Environ.* 15, 1891 (1981).
58. M. H. Conklin, G. R. Cass, L. C. Chu and E. S. Macias, "Wintertime Carbonaceous Aerosols in Los Angeles: An Exploration of the Role of Elemental Carbon," in *Chemical Composition of Atmospheric Aerosols: Source/Air Quality Relationships*, E. S. Macias, P. Hopke, Editors, Amer. Chem. Soc. Washington, D.C., 1981.
59. A. Hansen. The Use of an Optical Attenuation Technique to Estimate the Carbonaceous Component of Urban Aerosols. Annual Report, Lawrence Berkeley Laboratory Report, LBL 10735 (1980).
60. E. C. Ellis and T. Novakov. Application of Thermal Analysis to the Characterization for Organic Aerosol Particles. *The Science of the Total Environment* 23, 227-238 (1982).

61. J. R. Ouimette and R. C. Flagan. The Extinction Coefficients of Multicomponent Aerosols. Atmos. Environ. 16, 2405-2419 (1982).
62. A. Waggoner, private communication (1983).
63. S. H. Cadle, P. J. Groblicki and P. A. Mulawa. Problems in the Sampling and Analysis of Carbon Particles. Atmos. Environ. 17, 593-600 (1983).
64. R. L. Williams and D. P. Chock. Characterization of Diesel Particulate Exposure. General Motors Research Publication GM-3177 (1979).

APPENDIX A

THE IMPACT OF INCREASED DIESEL EMISSIONS ON VISIBILITY

1. In the year 2000, General Motors projects 25% of the light duty vehicles will be diesel powered (64).
2. General Motors projected "regional annual mean" particulate concentration due to light-duty diesels in the year 2000 is $10.5 \mu\text{g}/\text{m}^3$ for "Los Angeles Freeways" and $6.0 \mu\text{g}/\text{m}^3$ for downtown Los Angeles (64). The present calculation is based on $10 \mu\text{g}/\text{m}^3$ diesel particulate compared to an assumed 0% light duty diesel emission in 1981.
3. General Motors finds for diesel exhaust particulate, on average, 37% soluble material (77%w carbon) and 63% insoluble material (about 80%w carbon) (64). So in $10 \mu\text{g}/\text{m}^3$ diesel particulate, there are $2.85 \mu\text{g}/\text{m}^3$ organic C (C_o) and $5.0 \mu\text{g}/\text{m}^3$ elemental C (C_e). We assume all diesel exhaust particles to be in the "fine" particulate range.

4. Visual Range = $v_m = \frac{3.912}{b_{\text{ext}}}$

$$b_{\text{ext}} = b_{\text{ap}} + b_{\text{ag}} + b_{\text{sp}} + b_{\text{sg}}$$

where: b_{ext} = atmospheric extinction coefficient

b_{ap} = absorption by particles

b_{ag} = absorption by gases (essentially only NO_2)

b_{sp} = scattering by particles

b_{sg} = Rayleigh scattering by gases = $0.12 \times 10^{-4} \text{m}^{-1}$

5. Incremental increase in diesel particulate causes increase in both b_{ap} and b_{sp} . Based on Groblicki et al.(6):

$$\Delta b_{ap} \times 10^4 = 0.118 (\Delta C_e \text{ in fine fraction})$$

$$\Delta b_{ap} \times 10^4 = 0.118 (5.0) = 0.59$$

$$\Delta b_{sp} \times 10^4 = 0.044(1.2\Delta C_o) + 0.032(\Delta C_e)$$

$$= 0.044 \times 1.2 \times 2.85 + 0.032 \times 5.0$$

$$= 0.31$$

$$(\Delta b_{sp} + \Delta b_{ap}) \times 10^4 = 0.90$$

6. For downtown Los Angeles, the median yearly visual range for 1974-1976 was 7.5 miles (12.1 km)³(3), from which a median b_{ext} of $3.2 \times 10^{-4} m^{-1}$ is calculated. An increase of $6.0 \mu g/m^3$ of diesel particulate of the composition given above yields:

$$(\Delta b_{sp} + \Delta b_{ap}) \times 10^4 = 0.19 + 0.31 = 0.50$$

$$DOLA \text{ Mean Visual Range (Year 2000)} = \frac{3.912}{(3.2 + 0.50) \times 10^{-4} m^{-1}}$$

$$= 10.6 \text{ km}$$

$$= 12.4\% \text{ decrease relative to} \\ \text{1974-1976 mean}$$

7. In recent years visual range in Los Angeles and other California urban areas has been increasing. Accordingly b_{ext} has been decreasing. If this trend continued to the year 2000 except for the increment of b_{ext}

due to light diesel particulate then the decrease in visual range because of diesel car exhaust would be greater than calculated above (assuming no significant controls of diesel particle emissions).

APPENDIX B

Two MRI Model 1560 integrating nephelometers, modified by Professor A. Waggoner, were obtained from the University of Washington. One unit was designed to heat the inlet air to provide a measure of b_{sp} ascribable to dry particles. The second unit intended to measure b_{sp} at ambient temperature, was equipped with an external blower (28 cfm) to provide a shorter residence time within the sampler. In addition, the light source was heat shielded, and the unit was equipped with two constant current/temperature transducer (Radio Shack LM 334) to provide simultaneous measurement of the temperature in the sensing volume and that of the ambient air. The intention was to maintain a low ($\leq 1.5^{\circ}\text{C}$) ΔT between inside and outside air during sampling.

The transducers had a linear increase in voltage output with increase in temperature, 11.9 mV per $^{\circ}\text{K}$. The voltage difference between the transducers was monitored continuously to assess the ΔT . Both nephelometers were operated vertically in an air conditioned van, and the sampling was done through ducts shielded from solar heating and covered at their outlet with nylon stockings to exclude bugs and debris. The nylon stockings were cleared periodically to minimize fine particle loss. For the ambient temperature unit, the portion of the duct within the van was insulated. The heated nephelometer employed a tube heater on the sample line immediately ahead of the sampler. The temperature increase was monitored with mercury thermometers, one just ahead and one following the heater. The temperature difference was recorded periodically. The units were zeroed and calibrated with Freon 12 every 24 hours following a modified procedure provided by A. Waggoner.

Span drift between calibrations averaged 2%. At the three locations the mean difference between the outdoor temperature and that inside the ambient temperature nephelometer was $1.8 \pm 0.8^{\circ}\text{C}$. The average temperature difference across the heater on the inlet of the heated nephelometer was $16 \pm 1.6^{\circ}\text{C}$.

APPENDIX C

EVALUATION OF METHODS FOR ABSORPTION COEFFICIENT MEASUREMENT

A. Integrating Plate Method

1. Experimental

A Beckman Model B spectrophotometer was modified by inserting a platform in the sample compartment to support the sample, optical Neutral density (ND) filter and opal glass (see Fig. 2, p. 26a). By standing the spectrophotometer on end, the platform sample and other components were horizontal. A collimating f/1 lens beneath the platform was used to focus the light penetrating the opal glass onto the detector. The optics of the spectrophotometer provided a rectangular beam of cross section 2.2 cm x 0.15 cm upon entry into the sample compartment, decreasing to about 0.6 cm x 0.3 cm at the detector. The platform positioned the sample to provide a beam 1.3 cm x 0.2 cm, a relatively large beam area which permitted analysis of either 47 mm or 25 mm diameter filter samples.

The light source and detector provided peak response at 535 nm. The intensity profile was identical at different slitwidths indicating adequate resolution. Section 5 details modifications to the equipment to improve performance.

2. Precision of Transmittance Measurements

Imprecision in measurements with filters can result from spectrophotometer drift, lack of uniformity of the particle loading, variability in the degree of flatness of the filter, inhomogeneity in the filter material, and uncertainty in flow measurements. The short-term (< 10 min) drift in the spectrophotometer was measured by

repeated readings of transmittance through the opal glass alone or with blank filters plus the other components, without movement of the sample or opal glass. Coefficients of variation ranged from 0.2 to 1.5%. Repositioning the opal glass showed no increase in C.V. indicating the glass was homogeneous.

Employing blank Nuclepore filters, the C.V. for repeated measurements (the filter being removed between measurements) was \leq 1.8%. Individual blank Nuclepore filters showed no measurable variability across the filter surface.

Efforts to improve precision included use of a weight around the periphery of the filter and covering the filter with a microscope slide. The peripheral weight yielded no improvement. The use of the microscope slide did improve precision, but may disturb the sample when using loaded filters.

The Nuclepore filters used in this work exhibited about 58% transmittance, (using an ND filter and opal glass), independent of wavelength in the range 500-550 nm. The observed blank filter transmittance, relative to that for the opal glass set equal to 100%, varied with position between light source and detector, emphasizing the need for reproducible sample geometry.

Variability in the transmittance of Nuclepore filters within a batch would decrease precision with atmospheric samples unless blank values are obtained for each filter. However, for 5 filters the C.V. for transmittance was \leq 2%, suggesting that variability between filters did not contribute significantly to measurement imprecision. However, recent work with a greater number of filters demonstrated variations in filters, within a batch, which slightly exceeded the measurement imprecision. Furthermore, substantial differences between filters from different batches were found. Thus blank values were measured for each Nuclepore filter used in atmospheric sampling.

Variability in reading the transmittance of loaded filters was measured using atmospheric samples collected with 47 mm, open-face Nuclepore filter holders, without particle-size segregation. These holders yield a grid pattern in the particulate matter corresponding to the pattern of the plastic filter support. To eliminate this grid pattern and the possible resulting optical inhomogeneity, Nuclepore filter samples were also collected with a glass fiber or cellulose filter backing. A total of 15 filters were loaded without filter backing and six readings made for each filter. The precision for the filters ranged from 0.3 to 1.4% (C.V.), for samples collected with or without backing, covering a transmittance range from 53% to 92% (relative to a blank filter). The precision was also shown to be unchanged when the N.D. filter or collimating lens were removed, the wavelength was changed from 535 to 550 nm, if the N.D. filter was changed to provide 80% rather than 50% attenuation, or the sample position between light source and detector was changed (multiple readings then being made at the same position). Thus the variability with loaded filters reflects only that observed with blank filters (i.e. that ascribed to instrument drift).

The overall precision to measure b_{ap} including the variability in atmospheric sampling, was determined by parallel collection with three 47 mm open-face Nuclepore filters without size segregation. All sampling was for 120 minutes at 40 Lpm, providing 4.8 m³ air samples. Back-up filters eliminated the grid pattern discussed above. Different types of back-up (or support) filters were tried to assess the impact of such differences on precision. The results (Table C-1) show C.V. values within the range observed for blank filters indicating the three samplers to be equivalent, within experimental uncertainty. To illustrate the effect of such variability on b_{ap} values, a reading of 77.0%T (C.V. = 1.5%), corresponds to a b_{ap} of $(0.676 \pm 0.043) \times 10^{-4} \text{ m}^{-1}$ or a C.V. of 6.4% in b_{ap} measurement, based on a 4.8 m³ air sample.

TABLE C-1

PRECISION OF PARALLEL SAMPLING FOR b_{ap} MEASUREMENT

<u>Sample Set^a</u>	<u>Mean % Transmittance^b</u>	<u>C.V. (%)</u>
1 ^c	76.4	1.3
2 ^d	76.6	1.7
3 ^e	77.0	1.5
4 ^e	95.2	1.4
5 ^e	77.4	0.5

^aEach set includes three filters sampling in parallel.

^bWith ND-3 filter at 535 nm, particles facing the light beam. Average of 3 to 10 readings.

^cTwo units used glass fiber back-up filters and one unit, cellulose.

^dTwo units used cellulose back-up filters and one unit, glass fiber.

^eAll units used glass fiber back-up filters.

3. Factors Influencing Accuracy

Although the precision of transmittance measurements was relatively invariant with measuring conditions (for a given sampling geometry), numerous factors influenced the magnitude of these measurements. Of concern here are those factors which influenced the ratio of transmittance values for loaded and blank filters, since these will alter calculated b_{ap} values.

a. Microscope slides covering particle-loaded filters

Microscope slides placed on top of the Nuclepore filters were tried to improve their flatness. Without Nuclepore filter or opal glass, a slide reduced transmittance by about 8%. However, a slide placed on top of a blank Nuclepore filter or opal glass plate caused only 4 to 6% attenuation relative to the transmittance without the slide. This suggests that the microscope slides acts as both an attenuator and as a source of multiple reflection. Loaded Nuclepore filters (plus opal glass) with and without a microscope slide covering the filter yielded the results shown in Table C-2. At low particulate loadings the difference was insignificant but increased with increased loading (decreased transmittance). Assuming six-hour sample collection at 8 Lpm with a 47 mm filter, a change from 73.5 to 71.5% T would correspond to a change from $1.41 \times 10^{-4} \text{ m}^{-1}$ to $1.54 \times 10^{-4} \text{ m}^{-1}$ in b_{ap} . Since the improvement in precision provided by the microscope slide was slight, we conclude that such slides should not be used for b_{ap} determination.

b. Neutral density filters

Two ND filters, 52 mm diameter Vivitar ND-3 and ND-6, with anti-reflection metal oxide coatings on both surfaces, were tested. The rim around each of these filters prevented direct contact with the opal glass, leaving about a 2 mm spacing. The

TABLE C-2

EFFECT ON TRANSMITTANCE OF OVERLAYING LOADED NUCLEPORE FILTER WITH A
MICROSCOPE SLIDE

<u>Sample No.</u>	<u>Mean %T^a</u>	
	<u>Without Slide</u>	<u>With Slide</u>
1	94.0	93.5
2	89.4	88.3
3	73.5	71.5

^aTransmittance measured relative to that for a blank filter with or without microscope slide, as appropriate. Measurements made at 535 and 550 nm. No N.D. filter used. Particles face light source.

transmittances at 500-550 nm of the ND-3 and ND-6 lenses were 52 and 80%, respectively, employing either a collimated or diffuse light source. Thus the behavior of these filters differed from that of both microscope slides and blank Nuclepore filters in that they served as simple attenuators (i.e. did not cause multiple reflection).

Table C-3 demonstrates the effect of inserting the ND-3 filter between the Nuclepore filter and opal glass. The transmittance of loaded filters, relative to blank Nuclepore filters, increased by 1.6 to 3.9% T. The direction of change is predictable from the model previously given; by strongly attenuating reflected light, each particle has only one opportunity for light absorption, thus increasing the observed transmittance. The ND-3 and ND-6 filters were compared and found to produce the same change in transmittance with loaded filters.

c. Orientation of particulate matter relative to light source

The two faces of Nuclepore filters differ in surface roughness. Microscopic studies as well as extinction measurements have generally employed the smoother surface for sample collection. This practice was followed for the present study.

In the original IPM of Lin, the loaded filter was oriented such that the particles were sandwiched between the filter and opal glass. It was subsequently found that the optical depth was

TABLE C-3

EFFECT OF NEUTRAL DENSITY FILTER ON % T OF LOADED FILTERS

Sample ID	% Transmittance ^a				Δ of Mean
	Without ND-3		With ND-3		
	mean	C.V. (%)	mean	C.V. (%)	
N3	84.5	0.67	86.1	0.61	1.6
G3	84.1	1.02	86.4	0.35	2.3
W3	83.7	0.70	86.1	0.20	2.4
N4	72.3	1.00	76.1	0.89	3.8
W4	71.0	0.99	74.9	0.91	3.9
G4	70.6	0.65	74.4	0.28	3.8
W6	57.1	1.43	59.9	0.73	2.9
G6	56.9	0.73	60.1	1.42	3.2
N6	51.4	0.76	55.3	0.57	3.9

^aMean values for 3 to 6 determinations measured at 535 nm relative to blank Nuclepore filters representing 100% T. Particles face light source.

increased by multiple reflections through the particle deposit. Facing the particles toward the light source was reported to minimize this effect (43, 57).

Table C-4 compares transmittance values measured with the two orientations, with and without an N.D. filter. Using an N.D. filter, the % T reading was independent of orientation at low particle loading (high % T). At higher loadings, differences up to 4% T were seen, with higher values with particles oriented upward, consistent with a decrease in multiple reflections through the particles. Without the ND filter, the transmittance readings differed even at the lowest particle loadings, the difference increasing to about 10%T at higher loadings.

Based on the present results an N.D. optical filter and a particulate filter with particle orientation toward the light source were used for all IPM measurements. Except where noted, all measurements in this report employed this orientation.

d. The effect of filter particulate loading

The IPM is rigorously accurate only if particles have a single opportunity to absorb light and are located as discrete particles on the filter. Accordingly, particle loadings < 20 $\mu\text{g}/\text{cm}^2$ are recommended, but the upper limit must obviously depend on the aerosol composition. Employing atmospheric particulate samples collected without size segregation in Emeryville, adjacent to a street with moderate traffic, approximate loadings and the corresponding % Transmittance values are as follows: 7 $\mu\text{g}/\text{cm}^2$ (94.5 % T), 11 $\mu\text{g}/\text{cm}^2$ (77% T), 41 $\mu\text{g}/\text{cm}^2$ (59.7% T). Atmospheric sampling at three sites was done in parallel at two face velocities to provide optimal samples and a direct determination of the effect of loading on b_{ap} measurement.

TABLE C-4

EFFECT OF PARTICLE ORIENTATION ON % T^a

Sample ID	With ND-3 filter				Without ND Filter			
	Partic. Up ^b		Partic. Down		Partic. Up ^b		Partic. Down	
	Mean	C.V. (%)	Mean	C.V. (%)	Mean	C.V. (%)	Mean	C.V. (%)
4	94.8	1.2	94.5	1.7	94.2	1.0	90.6	1.2
5	77.2	0.3	73.0	0.4	75.2	0.7	65.5	0.6
6	77.6 ^c		73.4 ^c		73.0	0.7	64.7	1.7

^aMeasured at 535 nm relative to blank filters in same orientation.
Except as noted, means are for three trials.

^b"Up" indicates particles oriented toward the light source (see Fig. 2 p.26a).

^cSingle trial

e. The effect of wavelength

The effect of varying wavelengths from 450 to 600 nm was measured with a lightly loaded (86% T) and a heavily loaded (60% T) filter, relative to a blank filter under the same conditions. With the ND-3 filter, the lightly loaded sample showed no change in transmittance. The heavily loaded filter (probably exceeding the 20 $\mu\text{g}/\text{cm}^2$ limit) showed a 5% decrease in % T changing from 550 to 500 nm.

4. Interlaboratory Comparison of Results

Three 25 mm Nuclepore filters, loaded with atmospheric particles, were obtained from R. Weiss, University of Washington. The filter surfaces were curved concave upward, and the non-planarity was expected to decrease precision. Both laboratories measured the samples with and without ND filters. The results are shown in Table C-5, and indicate agreement between laboratories within one σ of AIHL's findings. The precision with these 25 mm filters was similar to those with 47 mm filters previously discussed. Multiple readings were considered essential with these samples to achieve acceptable precision.

TABLE C-5

INTERLABORATORY COMPARISON OF IPM (% T)^a

Sample	Wavelength	With ND ^b			Without ND ^b		
		Mean	AIHL C.V. (%)	UW	Mean	AIHL C.V. (%)	UW
1	535	96.4	0.6		94.0	0.8	
	550	96.0	1.2		94.0	1.1	
	520-550			97			94
2	535	92.3	0.9		89.0	0.4	
	550	92.7	0.8		89.9	0.7	
	520-550			93			90
3	535	79.3	1.1		73.3	0.8	
	550	80.3	1.2		73.7	1.6	
	520-550			80			75

^aThe means are averages of 7 to 14 readings. Particles face light source.

^bND = neutral density filter.

5. Modification of the IPM

Based on the above work, the technique was refined to improve precision as follows: (1) A line voltage regulator was added, (2) Vivitar neutral density (ND) optical filters were replaced by Rolyn ND filters, (3) the opal glass supporting the ND filter and Nuclepore filter sample was secured directly over the detector of the spectrophotometer rather than being supported by a platform. Unlike the Vivitar filters, the Rolyn ND filters have no rims and, therefore, were in direct contact with the supporting opal glass plate. This changed the location of the filter sample, reducing the rectangular light beam dimensions from about 2 X 13 mm to 2 mm by 5 mm.

With these modifications, instrument drift, measured by the mean differences in duplicate transmittance readings over about 10 min. period for blank Nuclepore filters, ranged from 0.18 to 0.34%T for four batches of filters. Over a period of several hours the mean difference between replicates was 0.6 to 0.9 %T. For both experiments the transmittance was adjusted to a value of about 100% for the initial measurement.

6. Variability

The modified equipment outlined above was used for all measurements in this atmospheric sampling study.

The variability in transmittance values between clean filters within a filter batch was measured to determine the need for measurement of blank values for each filter. With four batches of filters the range in %T within a batch was from 1.3 to 5.8%. Thus it was deemed essential to measure the transmittance value for each filter. Small differences between batches in average transmittance were also observed (Table C-6).

TABLE C-6

BATCH-TO-BATCH VARIATIONS IN MEAN TRANSMITTANCE VALUES FOR 0.4 μ M
PORE SIZE NUCLEPORE FILTERS

<u>Batch</u>	<u>Mean %T^a</u>	<u>N</u>
81C8D19	97	34
81N9C50	100	37

^ameasured relative to batch 81BOB79 equal to 100% T.

The precision of b_{ap} measurements, including the variability in sampling, was assessed with three, 47 mm co-collected Nuclepore samples, each sampling 4.8 m³ of outdoor air in Emeryville. The mean transmittance results were 75.9 ± 1.0 %T corresponding to a b_{ap} of $(0.80 \pm .04) \times 10^{-4} \text{ m}^{-1}$, or a C.V. of about 5%.

B. Evaluation of the Laser Transmission Method

1. Linearity

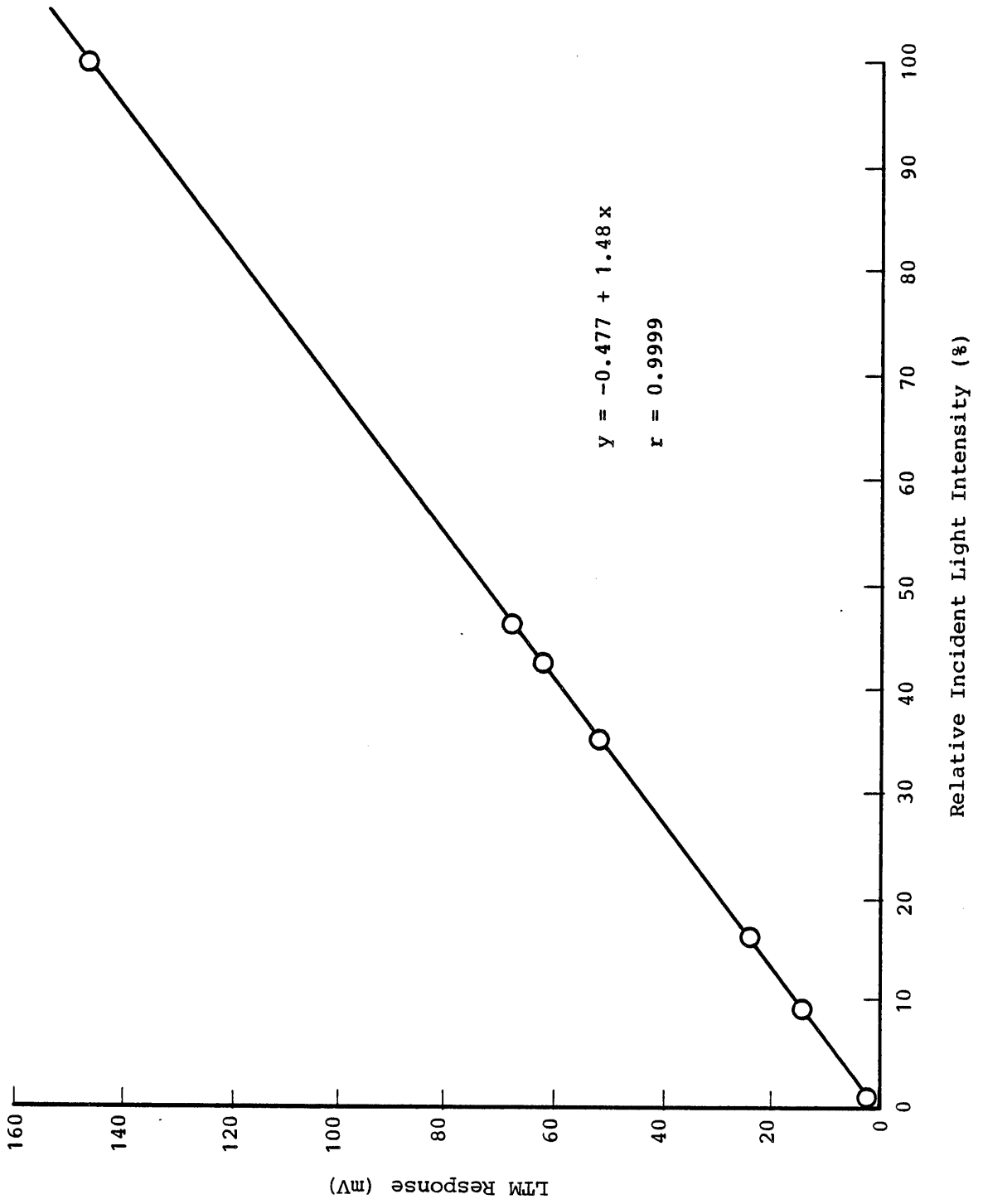
The linearity of the detector response was evaluated by inserting neutral density optical filters into the laser beam and recording the decreased response relative to that with only a clean quartz fiber filter in the light beam. The transmittance of the ND filters was established with a Beckman Model B spectrophotometer at 632 nm. The results (Figure C-1) show excellent linearity throughout the range relevant to loaded quartz samples.

2. Precision with Blank Filters with the LTM Method

The LTM method illuminates a filter area of about 1.2 cm diameter (1.1 cm²), or about 9% of the loaded filter area. Variations in filter density could produce substantial uncertainty in the filter blank for a given filter, since precise re-positioning of the loaded filter is not practical. To assess the uniformity in transmittance of blank filters, six blank Millipore (type RA) and eleven blank quartz (pre-fired Pallflex Quartz 2500 QAO) filters were each measured at five locations around each 47 mm filter disc.

Transmittance measurements were made at 633 nm with the Beckman Model B spectrophotometer which illuminated a filter area of 2 mm by 5 mm (1.0 cm²). The mean C.V. for the 5 measurements on each filter was 1.2% for both filter types. Thus, these data give no

Figure C-1 Linearity of LTM Detector Response



indication of substantial inhomogeneity within individual clean filters.

For a set of eight clean Millipore filters, the LTM detector output, which is proportional to %T, ranged from 80.7 to 85 mV. For 140 quartz filters the response ranged from 149 to 174 mV (mean 160.9 ± 6.6 mV). Thus it was judged necessary to measure blank values for each filter used for atmospheric sampling.

To assess the precision of measurement over a several-hour period, four blank Millipore filters were repeatedly measured. The coefficients of variation for the four filters for the replicate readings ranged from 0.33 to 0.44% (n=13).

Over the initial several weeks of instrument operation absolute readings for blank filters were observed to drop about 8%, suggesting a change in laser output intensity. Thereafter, the laser output was relatively stable. Measurements of both blank and loaded quartz filters were made relative to values for a common standard, four blank Millipore filters, measured the same day. Thus, no error in b_{ap} measurements should result from long-term drift.

3. Precision of b_{ap} Measurements

The precision of b_{ap} measurement, including the variability in sampling, and the influence of filter type, were assessed with three sets of co-collected Millipore and quartz 47 mm filter samples. Each sampled 4.8 m^3 of outdoor air in Emeryville. The mean transmittance results by LTM were $49.9 \pm 0.8\%T$ and $45.2 \pm 1.56\%T$ for Millipore and quartz filter samples, respectively. These corresponded to b_{ap} values of $(2.01 \pm 0.04) \times 10^{-4} \text{ m}^{-1}$ and

$(2.29 \pm 0.1) \times 10^{-4} \text{ m}^{-1}$, or C.V. values of 2.0 and 4.4%, respectively, the b_{ap} values differed by about 15% for the two filter types using the LTM method.

4. Interlaboratory Comparison of LTM Results

A series of Millipore type RA ambient air filter samples collected by the LBL staff in Fremont were analyzed by both the LBL and AIHL LTM units. The results, shown in Figure C-2 indicate excellent correlation. Agreement in response could not be expected since the voltage outputs depend on the degree of signal amplification which differed for the two units.

C. Further IPM and LTM Method Evaluations Comparisons

1. The Effect of Particle Orientation on Measurements by the IPM and LTM Methods.

To understand better the factors influencing the optical methods under study, the influence of particulate matter facing toward (up) and away (down) from the light source was determined using Nuclepore, Millipore and quartz filters with both the IPM and LTM methods. With the IPM methods, the evaluation was made for a loaded filter alone, (i.e., without opal glass or N.D. filter) loaded filter plus N.D. filter and opal glass, and loaded filter plus opal glass. The IPM employed a Beckman Model B spectrophotometer at 535 nm while the LTM operated at 633 nm.

Table C-6 summarizes the data obtained with six sets of simultaneously Nuclepore, Millipore and quartz filter samples, sampling in all cases at 40 Lpm for equal time periods (1-5 hrs). For ease in discussions, column numbers have been added at the bottom of the table.

Figure C-2 Comparison of AIHL and Lawrence Berkeley Laboratory LTM Instruments
Analyzing the Same Atmospheric Particulate-Loaded Millipore Filters

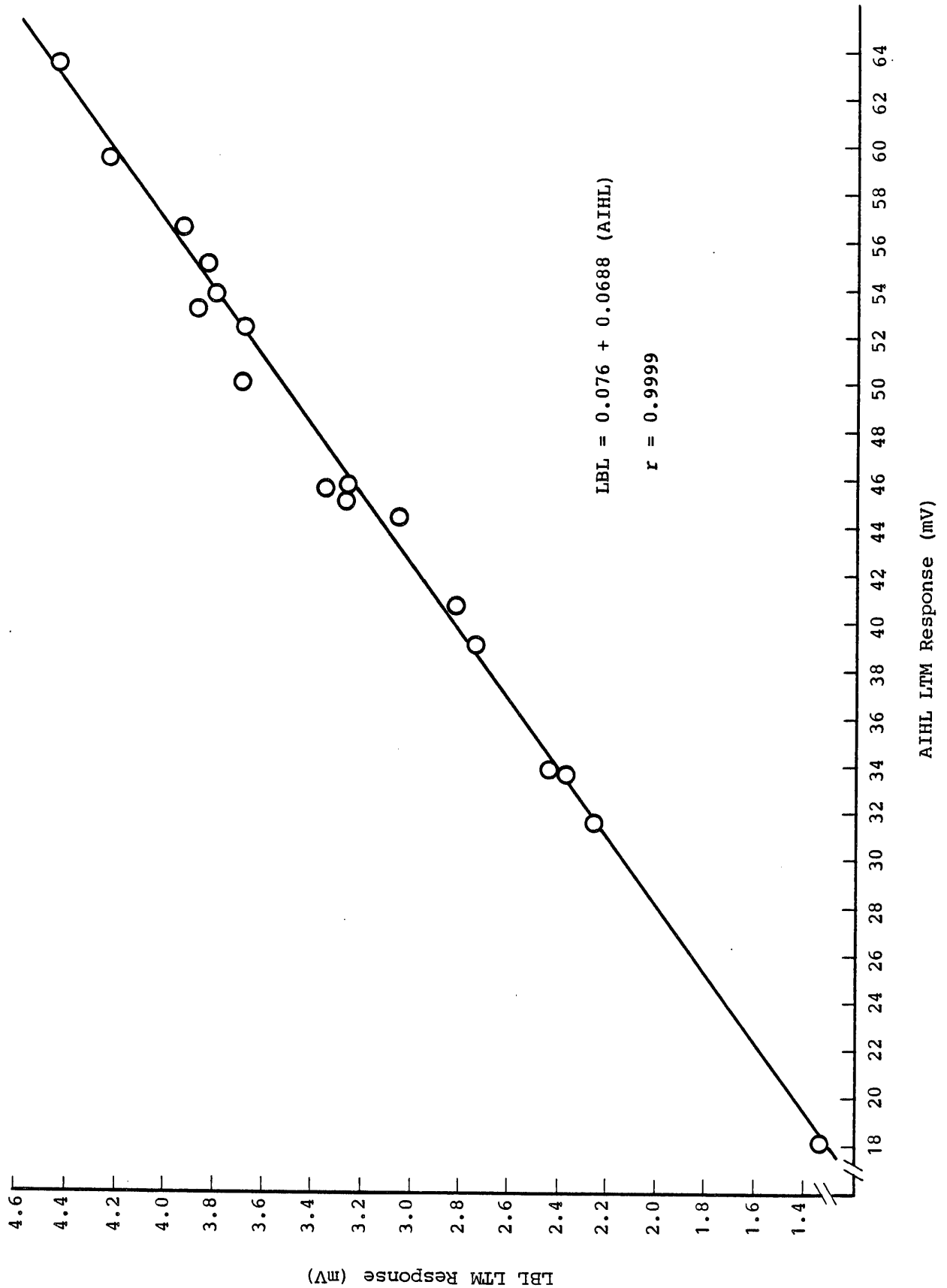


TABLE C-7
 INFLUENCE OF PARTICLE ORIENTATION WITH THE IMP AND LTM

% T (Beckman Model B)^a LTM (%T)^a

Sample Set	Orientation ^c	Nucleopore (NU) ND +		Millipore (M) ND +		Quartz (Q) ND +		Nu	M	Q				
		Alone	Opal	Alone	Opal	Alone	Opal							
A	up	85.7	87.3	87	87	62.9	62.9	61.7	61.0	82.3	69.2	67.0		
	down	86.0	85.3	82	82	62.7	60.2	59.3	59.4	82.6	68.3	67.5		
B	up	78.0	76.0	74.2	74.2	44.9	44.6	41.0	39.8	86.0	59.6	47.0		
	down	78.1	71.3	65.3	65.3	49.3	40.6	40.7	28.3	83.7	49.9	46.8		
C	up	78.0	76.7	75.0	75.0	45.0	44.0	39.0	38.0	83.5	50.0	44.2		
	down	77.5	71.5	65.0	65.0	43.2	39.3	37.5	27.3	83	49.6	44.6		
D	up	76.0	74.9	73.1	73.1	44.5	44.3	39.3	36.7	79.1	49.0	44.4		
	down	76.1	69.3	62.7	62.7	44.0	40.1	37.0	25.7	78.3	48.5	43.9		
E	up	71.3	67.4	65.3	65.3	37.5	33.7	27.0	25.7	76.8	49.3	32.8		
	down	71.3	61.3	55.5	55.5	33.0	29.7	26.0	17.0	80.3	39.9	32.4		
F	up	61.6	58.0	55.5	55.5	22.7	22.7	20.0	18.5	69	28.9	24.2		
	down	61.3	52.3	45.7	45.7	23.0	19.9	19.3	13.4	69.6	28.6	24.1		
Col. No.		1	2	3	4	5	6	7	8	9	10	11	12	13

a. Results expressed relative to those for the corresponding blank filter.
 b. Sampling times ranged from one to 5 hours.
 c. "Up" and "down" indicate toward and away from the light source, respectively.

Considering first measurements with the Beckman Model B, with loaded filter alone, the transmittance was independent of particle orientation up or down for the three filter types (columns 2,5, and 8). However, adding the opal glass caused a large decrease in transmittance when the particles faced away from the light source, i.e., when particles were in contact with the opal glass (columns 4,7 and 10). With the neutral density filter plus opal glass, the effect of orienting particles downward was qualitatively similar to that with only opal glass, but the differences up vs. down were much less.

The results are consistent with Weiss' conclusion (47) that the opal glass causes backward light scattering which produced multiple absorption by the particles on the filter in contact with it. Adding a neutral density filter sharply attenuated the backward scattered light from the opal glass, reducing the significance of multiple light absorption by particles by particles and, therefore, the difference with orientation.

Opal glass is reported to be necessary to correct for non-uniformly scattered light. Results with the present samples show a surprisingly small difference for the opal glass plus N.D. filter relative to the filter alone.

Comparing the degree of attenuation produced by the three filter types in the IPM (columns 3,6 and 9), equal particle loadings on Millipore and Quartz filters produced much lower transmittance values compared to loaded Nuclepore filters. This is consistent with multiple light absorption by particles which have penetrated significantly into these filters.

For the LTM, the trend with filter type is identical to that with the IPM (compare columns 11, 12, 13, to 3, 6 and 9). The Millipore and quartz filters, while probably promoting multiple absorption, are thought to function like the opal glass in the

IPM, aided by a large lens to focus more of the light scattered from particles on to the detector. With particles facing away from the light source (down), such effects by the filter should be minimized. Using Nuclepore, Millipore and quartz filters the differences with orientation are small and probably insignificant. Rosen believes that because penetration of particles into the Millipore and quartz filters is likely, no conclusion can be reached from these observations concerning the significant of light scattering from particles (42).

2. Wavelength Dependence of the IPM and the Difference Between the IPM and LTM

The IPM has typically been performed in the wavelength range 500 to 550 nm, close to the maximum in light sensitivity for the human eye. Our studies used 535 nm for maximum stability of the light source output. The LTM method, however, is fixed at 633 nm by the choice of laser (He-neon). To assess the contribution of the wavelength difference to the difference in b_{ap} values for the two methods, the IPM method was used at 535 and 633 nm with each filter type and compared to results for the LTM (Table C-8). In all cases, the particles faced the light source.

3. Conclusions

The results indicate that either the LTM or IPM method can be used to estimate b_{ap} values with acceptable precision. The reported accuracy of the IPM (i.e. $\pm 15\%$) and the factor of 3 difference between methods indicates that LTM results must be converted based on empirical correlations between methods.

TABLE C-8

INFLUENCE OF WAVELENGTH AND THE DISCREPANCY BETWEEN THE IPM AND LTM METHODS

Sample set	IPM (Nucleopore, %T)		IPM (Millipore, %T)		IPM (Quartz, %T)		LTM (%T at 633 nm)	
	535 nm	633 nm	535 nm	633 nm	535 nm	633 nm	Millipore	Quartz
A	87.3	88.1	62.7	67.5	61.7	65.0	69.2	67.0
B	76.0	78.5	44.6	50.1	40.0	45.2	50.6	47.0
C	76.7	78.9	44.0	49.5	37.8	43.2	50.0	44.2
D	74.9	77.3	44.3	50.1	38.0	41.8	49.0	44.4
E	67.4	71.1	33.7	39.2	26.6	30.6	40.3	32.8
F	58.0	62.7	22.7	27.8	20.2	23.0	28.9	24.2

APPENDIX D

CALIBRATION OF OPTICAL METHODS FOR ELEMENTAL CARBON

1. Preparation of Butane-Flame Carbon Samples

A procedure was adopted to provide elemental carbon standards with particle sizes relevant to those on atmospheric particulate filter samples. Carbon particles were generated from a butane flame employing a Mekker burner with the air inlet sealed to obtain fuel rich conditions. The carbon particles were drawn at a flow of 8-11 Lpm through a dry ice-isopropanol cold trap to remove water vapor and then into a 28 ft³ Tedlar bag. The bag was enclosed within an airtight box permitting a partial vacuum to be applied to the outside of the bag to draw in the airstream.

Particle size distributions for the particles in the bag exceeding 0.1 μm diameter were obtained with a Royco Model 226 laser aerosol particle counter.* Table D-1 shows results obtained about 5-hrs after filling the bag, and on the following day, immediately before and after loading filters with the suspended carbon particles. It can be assumed that particles $< 0.1 \mu\text{m}$ are present (and, therefore, not counted) although their relatively high coagulation rate should decrease their number with age.

Comparing the 5, and 18, and 21 hour particle concentrations and size distributions, nearly all particles $> 0.9 \mu\text{m}$ have been removed following overnight aging, presumably by sedimentation. Particle concentrations in the ranges 0.17-0.27 and 0.27-0.42 μm remained constant within a factor

*No attempt was made to recalibrate the Royco instrument for carbon particles. It is expected that the measured size distribution is too narrow, and the median diameter, too small.

TABLE D-1

SIZE DISTRIBUTION FOR CARBON PARTICLES^a

Particle Diameter, μm	Aged 5-hours		Aged 18-hours ^b		Aged 21-hours ^c	
	Particle Number ($\times 10^{-3}$) ^d	% of Total	Particle Number ($\times 10^{-3}$) ^d	% of Total	Particle Number ($\times 10^{-3}$) ^d	% of Total
0.10-0.17	3.15	0.6	12.7	9.7	13.1	13.8
0.17-0.27	14.0	2.6	16.2	12.4	20.5	21.6
0.27-0.42	60.5	11.4	43.7	33.5	33.5	35.2
0.42-0.62	82.2	15.5	38.2	29.2	19.5	20.5
0.62-0.87	90.6	17.1	15.0	11.5	6.5	6.8
0.87-1.17	84.5	15.9	3.9	3.0	1.6	1.6
1.17-1.52	66.9	12.6	0.8	0.6	0.3	0.3
1.52-1.92	49.9	9.4	0.1	0.1	0.1	0.1
1.92-2.37	29.0	5.5				
2.37-2.87	25.8	4.9				
2.87-3.42	12.4	2.3				
3.42-4.02	6.47	1.2				
4.02-4.67	3.31	0.6				
4.67-5.37	1.46	0.3				
> 5.37	0.9	0.2				

a. Results are uncorrected for calibration errors resulting from measurement of highly absorbing, non-spherical particles with the Royco Model 226 laser optical particle counter.

b. Obtained just prior to loading of filters.

c. Obtained immediately following loading of filters.

d. Mean results for three successive 30 sec particle counting periods.

of two, while those between 0.4 and 0.9 μm were substantially lower after overnight aging. The average of the 18 and 21 hour size distribution approximated a log-normal distribution (Figure D-1) with a number median diameter of 0.36 μm ($\sigma_g = 0.18$).

Carbon particles were loaded on 47 mm Pallflex 2500 QA0 quartz filters which had been prefired in air for 17 hours at 500°C to reduce their carbon blank values. Sampling was done at 10 Lpm for 5 sec to 8 min periods in a stainless steel filter holder. Samples ranged from a barely discernable (by eye) grey to nearly black.

To remove co-generated organic carbon, the samples were baked in air at 300°C for two hours and at 350°C for 1-5 hours. At 300°C no change in transmittance (i.e. blackness) was observed while at 350°C the filters became measurably lighter indicating that some elemental carbon was lost, together with the more readily oxidized organic carbon.

Electron micrographs of the filter samples revealed loose aggregates, generally exceeding 10 μm in diameter. Thus the particle size following collection bore no apparent relation to that while suspended in air.

2. Calibration of the LTM

The samples were measured for absorbance by the laser transmission method (LTM). Figure D-2 plots carbon levels against $-100 \ln(I/I_0)$ or "Attenuation". A high correlation is observed ($r = 0.992$). However, the slope of the least squares line (5.6 $\text{cm}^2/\mu\text{g}$), is about one third of that previously reported by the Lawrence Berkeley Laboratory with this method (59).

To elucidate the factors influencing calibration of optical carbon analyzers, samples collected by the Lawrence Berkeley Laboratory and

Figure D-1 SIZE DISTRIBUTION FOR AGED CARBON PARTICLES FROM A BUTANE FLAME

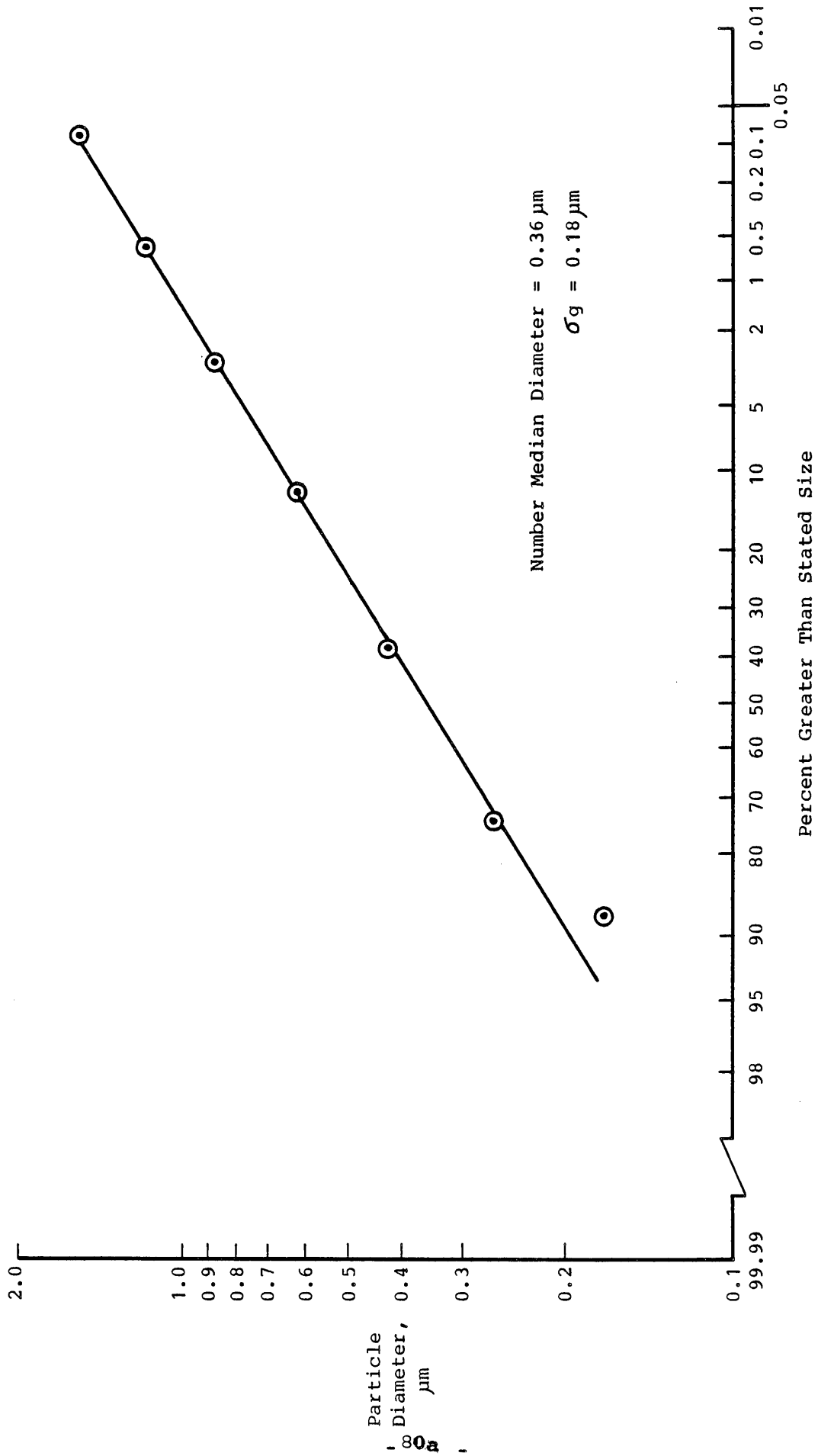
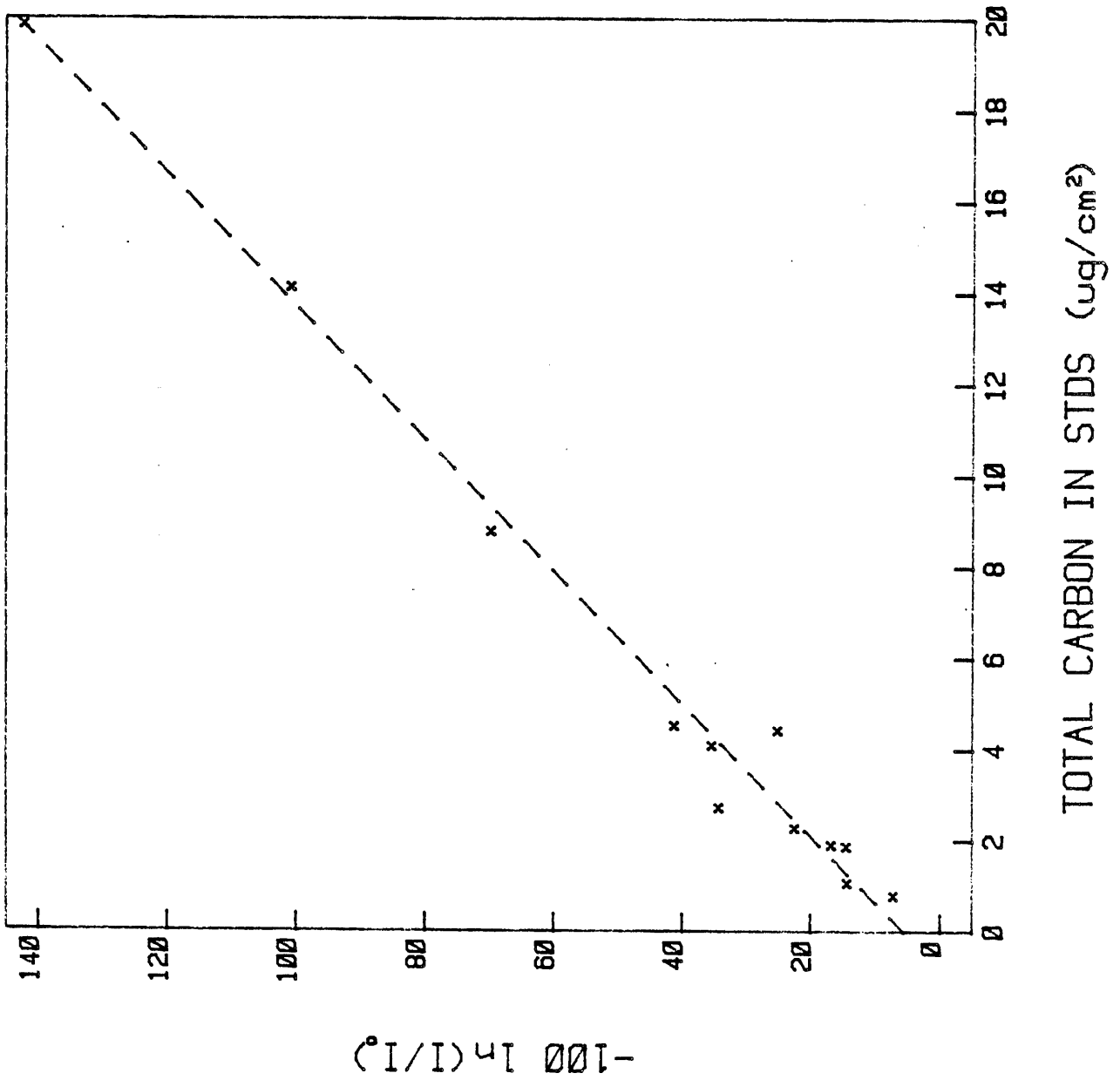


Figure D-2 Calibration of LTM with Aged Carbon Particles

LTM



100 100 100

analyzed by them for black carbon* were analyzed by the AIHL LTM. These samples included diesel soot, propane-flame derived soot, particulate matter collected in a motor vehicle tunnel and atmospheric samples. Comparing measurements of "attenuation" between laboratories, the agreement was excellent [AIHL-LTM = -4.03 + 1.02 (LBL-LTM) $r = 0.9983$, $n = 14$]. Calibration of the AIHL LTM with these samples is shown in Figure D-3. Excluding points above $11 \mu\text{g}/\text{cm}^2$, the mean slope, $23 \text{ cm}^2/\mu\text{g}$, is about four times that observed with the aged butane-flame carbon samples.

Variability in specific absorption (i.e. absorption per unit mass) for carbon particles has been frequently observed. Figure D-4 shows the variation in absorption efficiency, E , with graphitic carbon particle diameter for homogeneous spheres (density $2.0 \text{ g}/\text{cm}^3$, index of refraction $1.96 - 0.66 i$) and for loosely packed soot clusters which are still spherical (density $1.0 \text{ g}/\text{cm}^3$, index of refraction $1.56 - 0.47 i$). The results for loosely packed clusters exhibit a maximum of about $9 \text{ m}^2/\text{g}$ (or $9 \text{ cm}^2/\mu\text{g}$) at $0.2 \mu\text{m}$ diameter, compared to about $6 \text{ m}^2/\text{g}$ for homogeneous spheres. Both spheres and loose cluster show sharply decreasing efficiencies at larger size. The value, $5.59 \text{ cm}^2/\mu\text{g}$ for the butane-flame carbon from the present study is similar to literature values for pure carbon samples.

*Analyzed using a thermal analysis technique (60) which provided C_e and C_o values equivalent to the interlaboratory mean in the General Motors interlaboratory comparison of carbon analysis methods.

Figure D-3 Calibration of ITM With IBL Black Carbon Samples

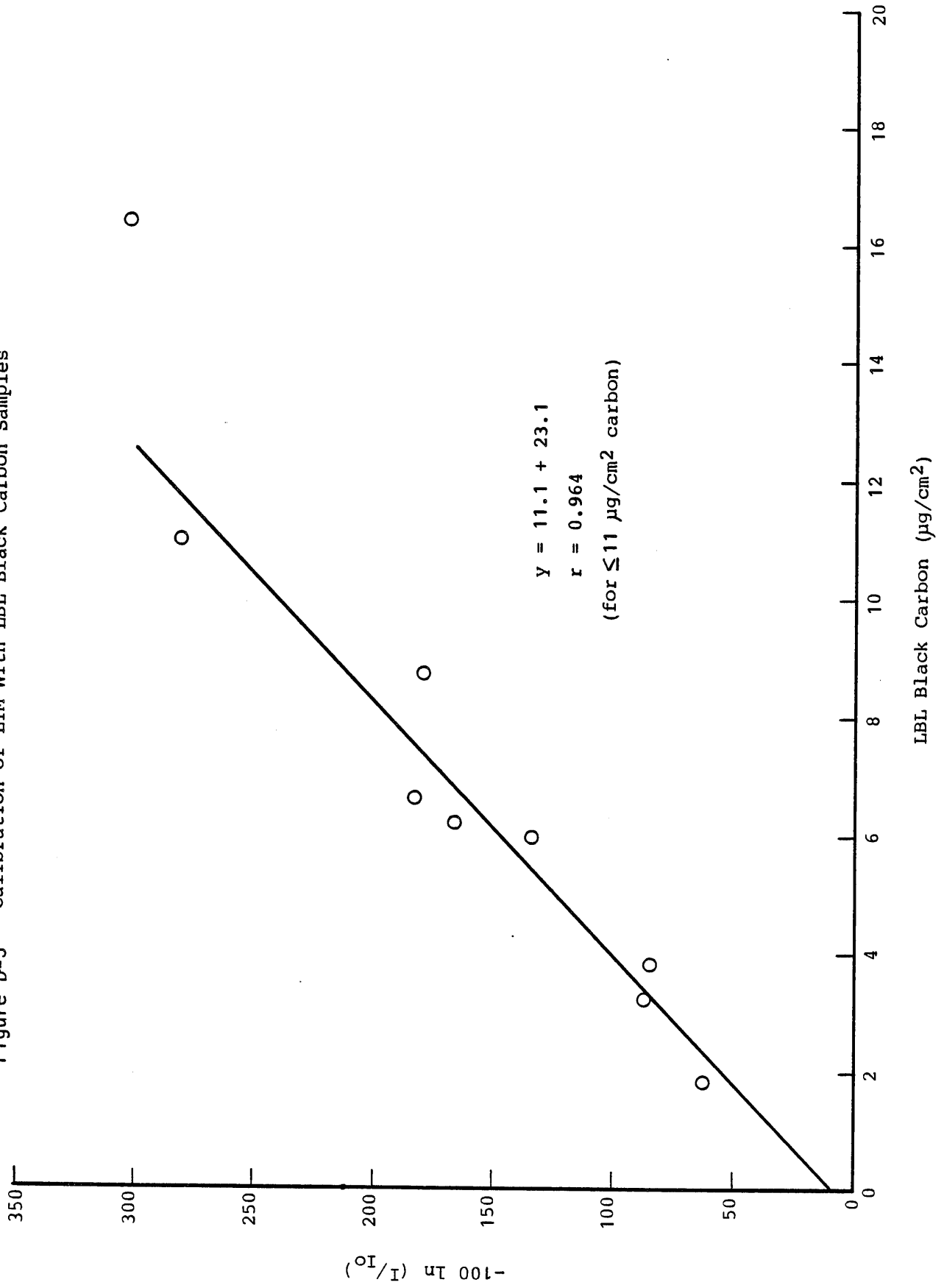
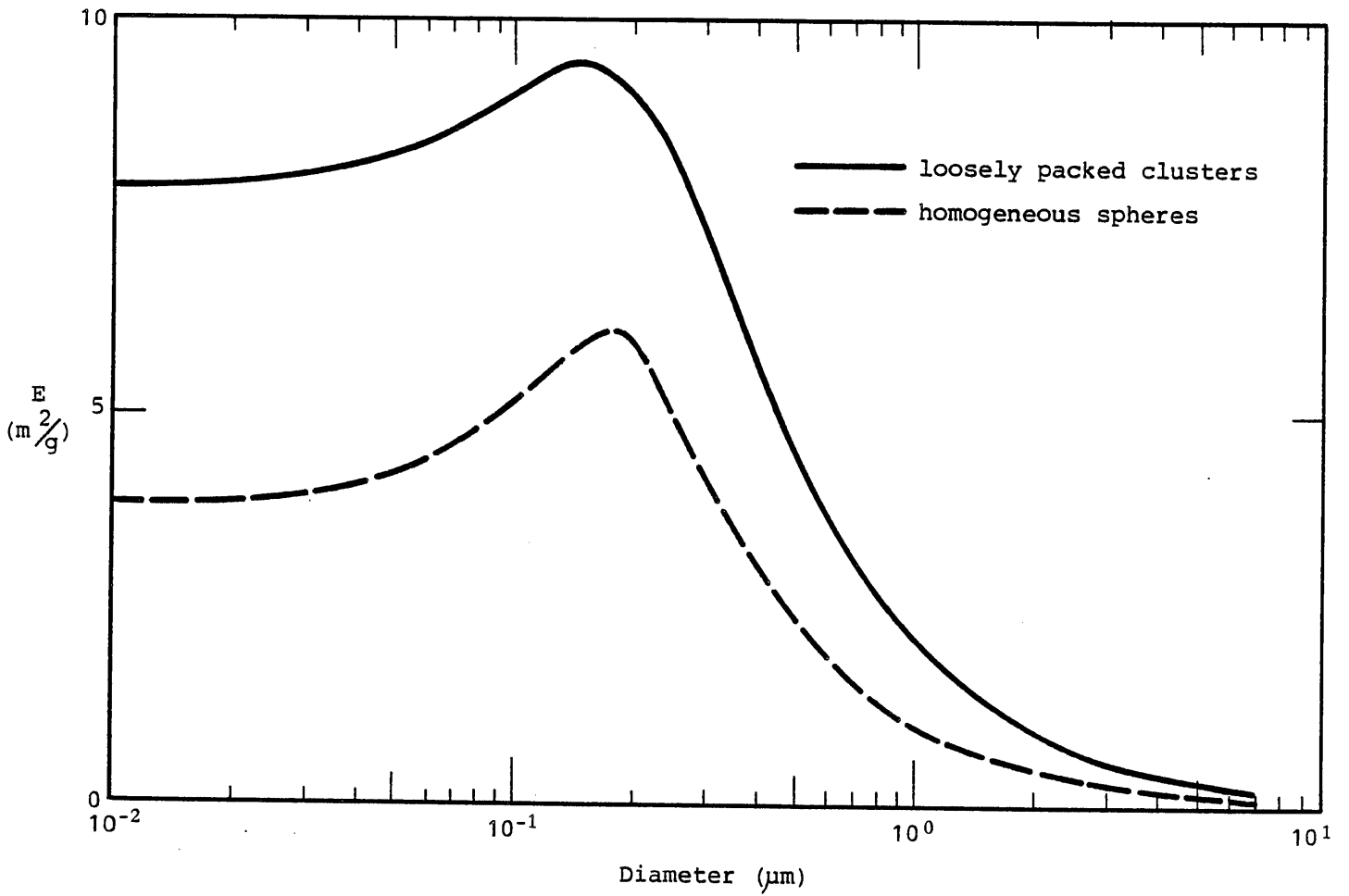


Figure D-4
LIGHT ABSORPTION EFFICIENCY FOR GRAPHITIC CARBON (SOOT)



Taken from Ouimette and Flagen (Reference 61)

In addition to variability with particle size, the absorption efficiency for particles penetrating into the mat of a filter can be enhanced by a factor of two because of multiple absorption. Waggoner considers this the likely reason for the high absorption efficiencies obtained with the LTM (62). It is, therefore, apparent that light absorption techniques for measuring C_e should be calibrated with the most relevant material and filter medium. For the present study, this is atmospheric particulate matter samples on quartz fiber filters which have been analyzed for elemental carbon by an independent technique. Since the size distribution of atmospheric carbon particles, before and after filter collection, is expected to vary with location and source, it follows that absorption methods can only be used to approximate the atmospheric C_e concentration.

3. Calibration of the Reflectance Method

Figure D-5 plots butane-flame derived carbon levels against $-100 \ln (R/R_0)$ measured with a Photovolt model 670 reflectance meter. R and R_0 refer to the reflectance of loaded and blank filters, respectively. The plot appears identical to that for the LTM for the same samples (indicating high correlation between $\ln (R/R_0)$ and $\ln (I/I_0)$) with a mean slope of 14.3. Thus a given carbon loading produced a greater decrease in reflectance compared to the change in absorbance with the LTM.

Employing the same technique previously used for linearizing the reflectance data (34), Figure D-6 illustrates the calibration of the reflectance method with the butane-flame carbon samples. For atmospheric samples in the range 3 to 21 $\mu\text{g}/\text{cm}^2$, this calibration yielded C_e values $19 \pm 3\%$ higher than our earlier calibration (34) which employed butane-flame carbon collected without significant aging. Considering the scatter in Figure D-6, the 19% difference is of doubtful significance.

The LBL black carbon samples were also used to calibrate the reflectance meter. The resulting calibration ($a = 0.037$, $b = 1.62$, $r = 0.9897$ for

Figure D-5 Calibration of Reflectance Meter With Aged Carbon Particle Samples

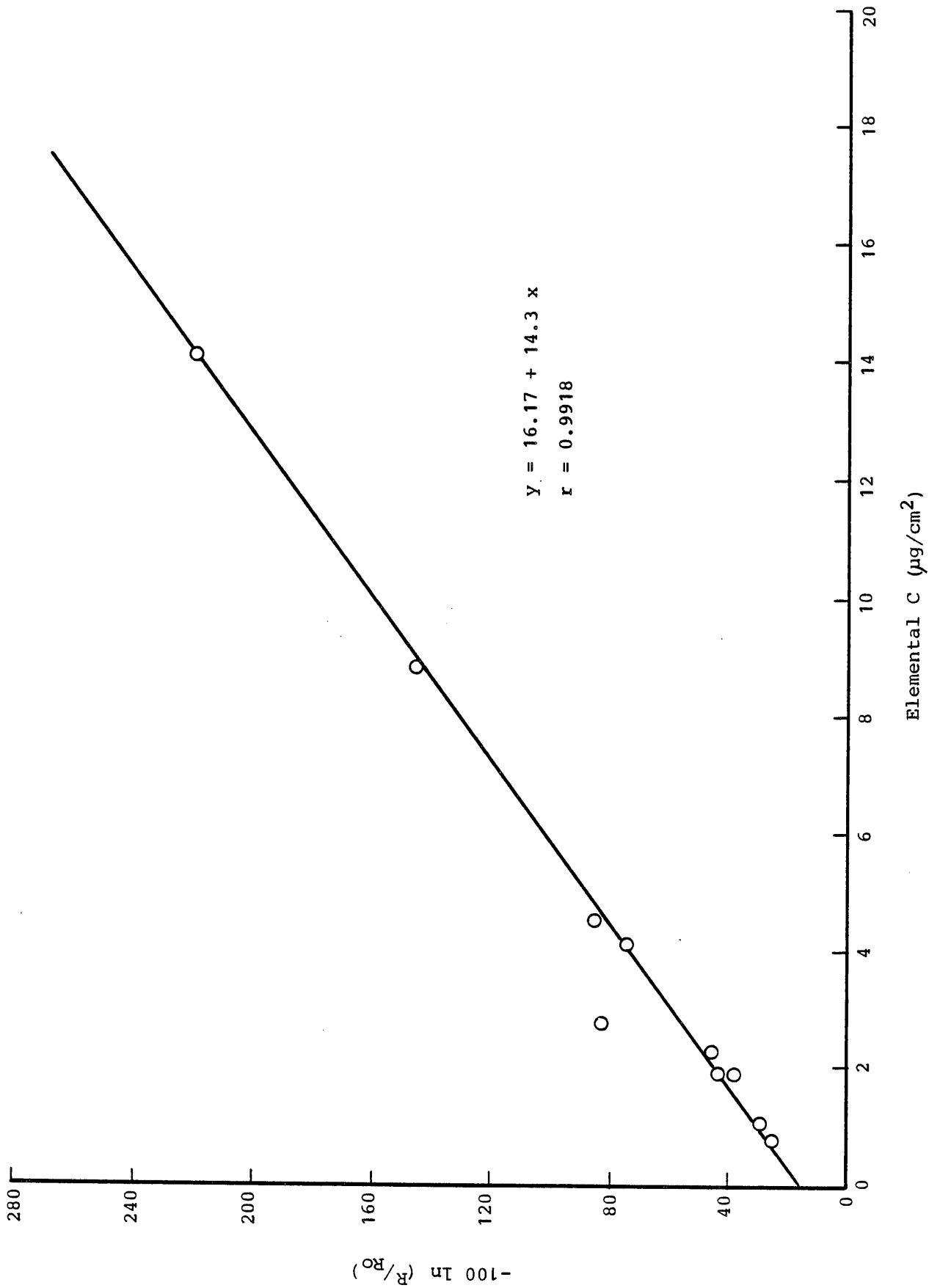
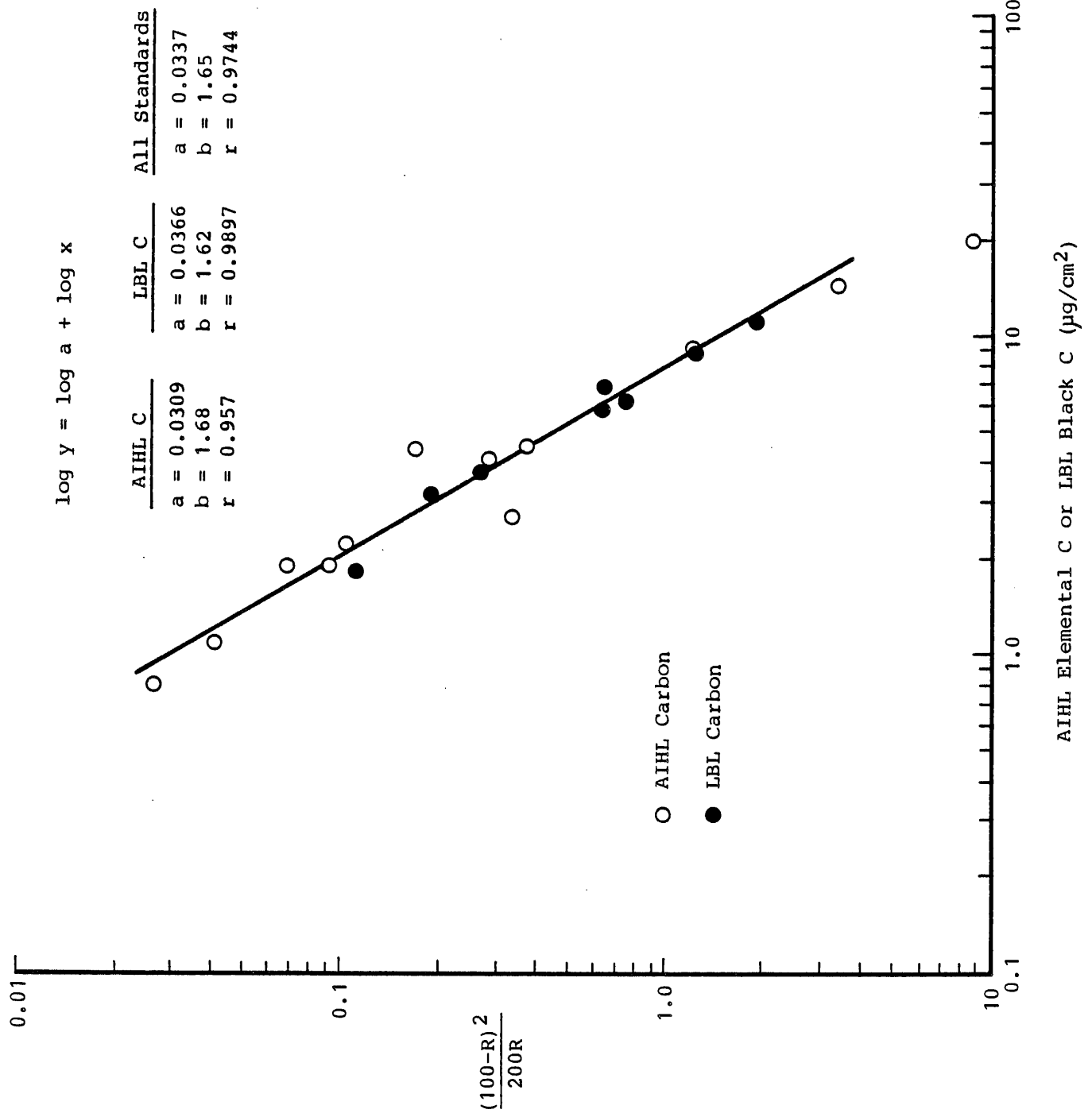


Figure 10-6

Calibration of Reflectance Meter
With Aged Carbon Particle and LBL Black Carbon Samples



the equation shown in Figure 15) yielded results for samples in the range 3 to 21 $\mu\text{g}/\text{cm}^2$ which differed, on average by 3.3% from those using the calibration obtained with the aged carbon particles. Thus the calibration of the reflectance meter is nearly invariant with the carbon used, in contrast to the calibration of the absorption method. Similar observations have been made elsewhere (62). This invariance has prompted our continued use of the reflectance technique, in spite of its inaccuracy with 24-hr filter samples (34).

4. Comparison of Current and Previous Reflectance (RM) Calibrations

As part of a previous study the RM was calibrated with butane flame-derived soot collected without aging, and baked at 20-30 Torr at ca. 250°C with a slow air bleed to eliminate co-generated organic compounds. Comparing the masses of the carbon standards needed for a given reflectance, the current calibration shows about 18% higher carbon loadings ($\mu\text{g}/\text{cm}^2$).

In an interlaboratory comparison using 24-hour hi-vol quartz filter samples, the RM provided C_e values which averaged 49% of the interlab mean. If the current RM calibration had been used, the RM values would represent 58% of the interlab mean. Thus calibration, alone, cannot account for the comparatively poor RM results obtained in the preceding interlaboratory comparison. The principal factor in providing better agreement in the current study probably the use of short-term (4-hour) samples, which minimized possible errors in the RM due to sample inhomogeneity.

5. Sensitivity of the Reflectance Method to the Calibration Curve Fitting Procedure

In addition to the linear regression equation for all data for the log-log curve shown on Figure D-6 (RM-4), the data points were fit with polynomial equations as well. The effect of curve fitting method was assessed by comparing calculated $\mu\text{g}/\text{cm}^2$ C_e for several curve fitting

options. Using a single ploynomial to fit all the data, the mean C_e was decreased by 3.5% (n = 109). Using a polynomial fit for only the lightly loaded standards (R > 60%), the mean C_e was reduced by 9.4%. For samples with R < 60, the difference was 1.6%.

APPENDIX E

MEASUREMENT OF AMBIENT TEMPERATURE AND RELATIVE HUMIDITY

D. Ambient Temperature

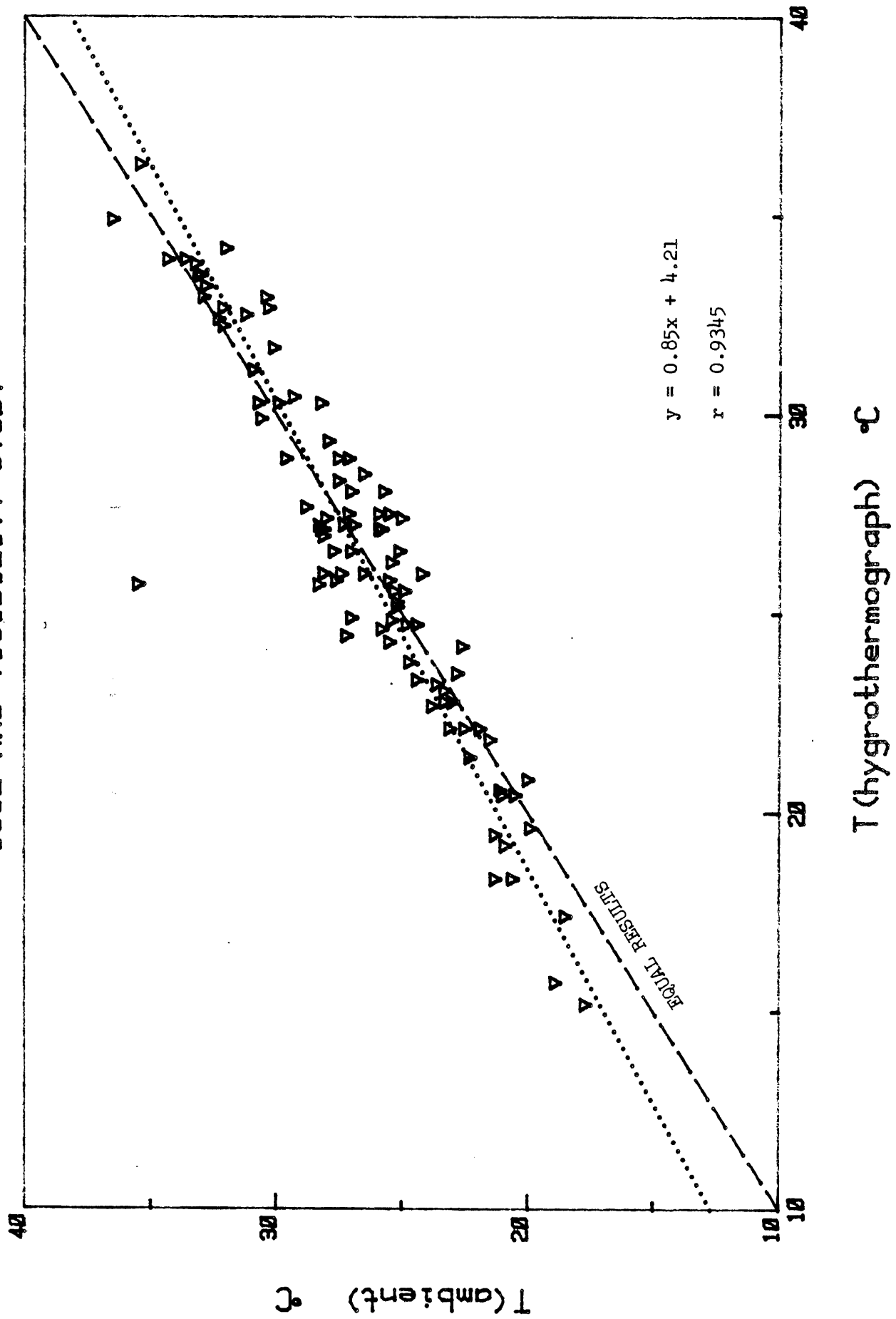
Ambient temperature determinations were needed to calculate relative humidity from dew point measurements and to aid in interpreting aerosol data. Ambient temperature (and relative humidity) were measured by a hygrothermograph located in the shade, adjacent to the sampling van. Where temporary shelters were used for shade, these were covered with aluminum foil to minimize solar heating. In addition, temperature was measured with a constant current/temperature transducer (LM 334), sensitivity 10 mV/°K. The sensor was located within the inlet hose of a nephelometer, about 30 cm from the end of the hose. The hose was carefully shielded to minimize solar heating. Figure E-1 compares temperature measurements by the two procedures. In the range 15-35°C, the mean difference was $0.2 \pm 1.7^\circ\text{C}$.

A dew point hygrometer operated satisfactorily for about half the sampling program. Using dew point values and ambient temperature measurements from the temperature transducer described above, relative humidity could be calculated. In addition a human hair hygrothermograph, calibrated against a sling psychrometer, operated satisfactorily throughout the program. Four-hour average results by the two techniques are compared in Figure E-2. In the range 30 to 70% R.H., the two techniques show agreement within 3% R.H. Because of the dew point hygrometer failure, hygrothermograph R.H. data were employed for data analysis.

TEMPERATURE COMPARISONS

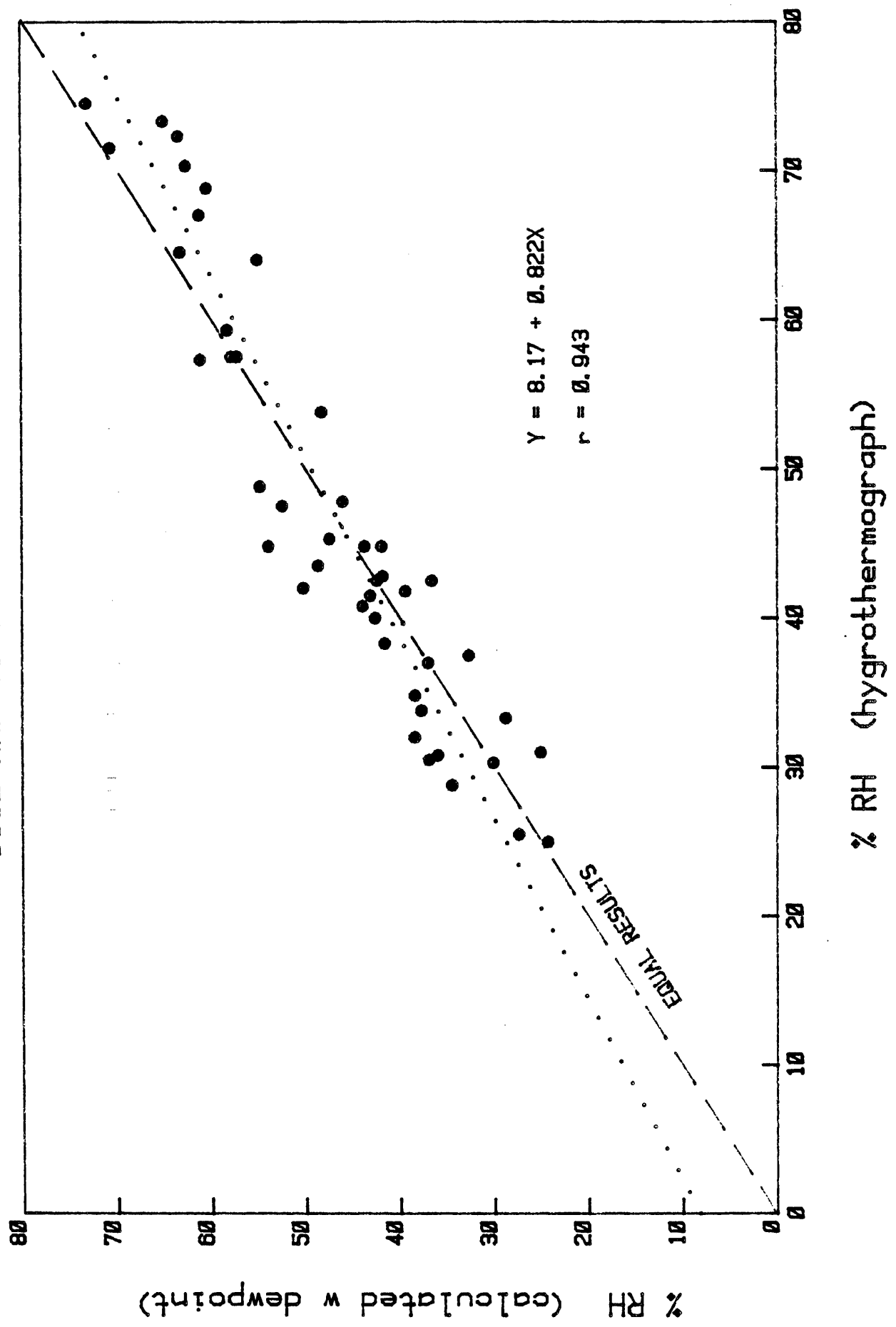
1982 ARB VISIBILITY STUDY

Figure E-1



RH COMPARISONS 1982 ARB VISIBILITY STUDY

Figure E-2



APPENDIX F

EXPERIMENTAL DIFFICULTIES WITH THE TRUE PARTICULATE CARBON MEASUREMENTS

The procedures followed were similar to those previously described (34,40) except as follows: (1) the filter medium used was pre-fired Pallflex 2500 QAO quartz fiber instead of pre-fired glass fiber, (2) the sampling time was 12 rather than 24-hours, (3) the denuder tubes were replaced after 72-hours sampling, (4) organic compounds were removed from the Al_2O_3 by elution with Me_2Cl_2 followed by 50:50 v/v $MeOH:Me_2Cl_2$ rather than by elution with Me_2Cl_2 , alone. The latter change was intended to provide more complete recovery of polar organics. However, with atmospheric samples the mixed solvent also led to the elution of water retained on the Al_2O_3 . Traces of water remaining following solvent removal decreased the precision in carbon measurements. The blank for solvent recovery from Al_2O_3 was 115 μg and 227 μg in two trials. However, eight atmospheric Al_2O_3 samples from Riverside had carbon levels by solvent extraction of $103 \pm 17 \mu g$.

As in earlier studies (40) generally over 50% of the total carbon was recovered from the fluidized bed implying the importance of volatilization following collection. However, in contrast to the earlier work, no correlation was observed between the apparent particulate carbon values (i.e., filter plus fluidized bed) and total carbon values with the hi-vol sampler. We conclude therefore, that the present fluidized bed data are probably not useful.

GLOSSARY

b_{ap}	absorption coefficient for particles
b_{ag}	absorption coefficient for particle gases
b_{sp}	scattering coefficient for particles
b_{sg}	absorption coefficient for gases (i.e., Rayleigh scattering)
b_{ext}	extinction coefficient
b'_{ext}	extinction coefficient excluding b_{sg}
C	coarse (e.g. CSO_4 indicates coarse sulfate)
C_e	elemental carbon
C_o	organic carbon
C_t	total carbon
F	fine (e.g. FSO_4 indicates fine sulfate)
IPM	integrating plate method
LTM	laser transmission method
LVC	low volatility carbon (particle plus vapor phase)
PC	particulate carbon
R	residual fine mass
RM	reflectance method
T	transmittance